

University of Reading  
School of Mathematics, Meteorology & Physics

Application of the Phase/Amplitude  
Method to the Study of Trapped  
Waves in the Atmosphere and Oceans

This dissertation is a joint MSc in the Departments of Mathematics &  
Meteorology and is submitted in partial fulfillment of the requirements for the  
degree of Master of Science

Dan Lucas

August 19, 2007

## Abstract

This work examines the numerical performance of the phase/amplitude or Milne's method over existing numerical techniques in the solution of the time independent Schrödinger equation eigenvalue problem. This method involves deriving a nonlinear ODE in phase or amplitude and implementing a fourth order Runge-Kutta solver with a shooting method to compute the eigenvalue and fit the boundary conditions. The Schrödinger equation in the context of equatorial waves and trapped lee waves is studied in cases where known analytical solutions exist and in cases where numerical techniques are the only method of solution. This work highlights the advantages of the phase/amplitude method over its contemporaries, those being efficiency in resonant mode searching and accuracy, particularly in higher modes.

*I confirm that this work is my own and the use of all other material from other sources has been properly and fully acknowledged.*

# Contents

<b>1</b>	<b>Numerical Method</b>	<b>4</b>
1.1	Deriving the phase/amplitude ODEs . . . . .	4
1.2	Solving the phase/amplitude ODEs . . . . .	6
1.3	Boundary Conditions . . . . .	8
1.3.1	Initial Conditions . . . . .	8
1.3.2	Boundary Condition at infinity . . . . .	10
1.4	Shooting Method . . . . .	11
1.5	MATLAB routine . . . . .	15
1.6	Alternative Numerical Methods . . . . .	15
1.6.1	Standard discretisation . . . . .	16
1.6.2	Direct Shooting Method . . . . .	17
1.6.3	WKB approximation . . . . .	18
<b>2</b>	<b>Equatorial Waves</b>	<b>20</b>
2.1	$\beta$ -plane Derivation . . . . .	20
2.2	Analytic Solutions . . . . .	22
2.3	Numerical Solutions . . . . .	23
2.3.1	Accuracy of $\lambda$ & Resolution . . . . .	25
2.3.2	Convergence . . . . .	26
2.3.3	Error in full Solution . . . . .	27
2.3.4	Initial Conditions . . . . .	29
2.4	Wave modes . . . . .	30

<b>3</b>	<b>Lee Waves</b>	<b>36</b>
3.1	The Linearised Boussinesq Equation Set . . . . .	37
3.2	Lee Wave Schrödinger Equation . . . . .	38
3.3	Analytic Scorer parameter profile . . . . .	40
3.3.1	Numerical Results . . . . .	43
3.4	Observed Scorer parameter profiles . . . . .	46
<b>A</b>	<b>MATLAB functions</b>	<b>54</b>
A.1	Phase/Amplitude routine . . . . .	54
A.2	Direct Shooting Method . . . . .	59
A.3	Matrix Eigenvalue Method . . . . .	63
A.4	Bessel function . . . . .	64

## Introduction

The study of many oceanographic and atmospheric waves can be reduced to understanding solutions of the time independent Schrödinger equation.

$$\frac{d^2y}{dx^2} + [V(x) - \lambda]y = 0 \quad (1)$$

where we denote  $V(x)$  as the potential and  $\lambda$  as the eigenvalue of the problem. The form of potential and the physical meaning of the eigenvalue is given by the type of wave motion under consideration, for example the eigenvalue often involves information about the wave motion normal to  $x$ . This ODE arose in the study of quantum mechanical systems and has been widely studied in this context.

This study will investigate regimes where the potentials  $(V(x) - \lambda)$  have a “turning point”, that is the transition from positive to negative values. Solutions in a region of positive potential have a wave-like behaviour and solutions in regions of negative potential exhibit exponential behaviour. Solutions of a second order ODE such as equation (1) have two independent solutions, thus in a region of negative potential these two solutions denote exponential growth and decay. Since it is not physically possible for waves to have infinite energy, only decaying waves can exist. Such wave motions correspond to trapped waves, this study will be concerned with two atmospheric/oceanographic trapped waves; lee waves and equatorial waves.

The numerical technique that is studied in this work is known as the phase/amplitude method or “Milne’s method” after the mathematician who first described it. This method has been widely used in the field of quantum mechanics but it has not, to date, been used in a meteorological context. This method looks for solutions under the form

$$y(x) = A(x)e^{i\Phi(x)}$$

where  $A$  and  $\Phi$  represent a phase and amplitude function that depends on coordinate  $x$ , a more physically appropriate formulation of solutions of the

Schrödinger equation. This transforms equation (1) into a nonlinear ODE to be solved for either phase or amplitude. It is not usual to replace the solution of a linear ODE with the solution of a nonlinear one, however solving for phase and amplitude in this way is a more physically realistic approach since wave motions in an inhomogeneous domain, i.e. where the potential varies with  $x$ , will have a phase and amplitude also dependent on  $x$ . We consider solutions over the interval  $[x_0, +\infty)$ , thus we require at least three boundary conditions to find a unique solution since formulating the solution in terms of phase and amplitude as above is non-unique (e.g.  $\Phi(x) = 0 \Rightarrow y(x) = A(x)$ ). A fourth order Runge-Kutta scheme is employed in the solution of the ODEs with a WKB type approximation to obtain initial conditions, at  $x_0$ , on phase and amplitude, which allow for smooth (non-oscillatory) solutions. The boundary condition “at infinity” is dealt with numerically by integrating to some extent past the turning point and a shooting method on  $\lambda$  is employed where an iterative process computes the eigenvalues for which resonance occurs. The eigenvalues are updated by solving the boundary condition via Newton iteration i.e. we wish  $y \rightarrow 0$  as  $x \rightarrow \infty$ .

The method is compared against known solutions and alternative numerical techniques; a direct shooting method (solving the Schrödinger equation with a fourth order Runge-Kutta scheme with a Newton solver fixing the boundary condition as in the phase/amplitude method) and a matrix eigenvalue method (discretising the problem as a system of second order finite difference equations and solving with an eigenvalue algorithm). The phase/amplitude and alternative methods are discussed in detail in chapter 1.

The oceanographic waves investigated in this work are trapped equatorial waves and are discussed in chapter 2. The  $\beta$ -plane shallow water equations are reduced to the Schrödinger equation in meridional wind with respect to latitude, where the potential is quadratic in latitude and the eigenvalue is in terms of zonal frequency and wave number. Waves are trapped about

the equator whilst propagating zonally around it. The analytic solutions in terms of parabolic cylinder functions presented by Matsuno (1966) [10] are used to test the methods.

The Schrödinger equation in the context of trapped lee waves is discussed in chapter 3. Here a linearised Boussinesq equation set is used to derive the Schrödinger equation for vertical wind speed with height, the potential in this case is the ‘Scorer parameter’, a function of mean horizontal wind speed and static stability with height. The horizontal wave number takes on the role of eigenvalue and resonance modes are computed from profiles of Scorer parameter. Known analytical solutions in terms of Bessel functions are used for comparison here, where the Scorer parameter profile is exponential. An observed profile of Scorer parameter is interpolated using cubic splines and the numerical methods are used to compute resonance modes.

Also included in this manuscript is a short section summarising the findings and an appendix with examples of the MATLAB code developed.

# Chapter 1

## Numerical Method

As mentioned in the introduction the method used in this study will be the phase/amplitude method and results in solving an ODE system using standard numerical integration (4th order Runge-Kutta) with a shooting method on  $\lambda$  to fix the end boundary condition.

### 1.1 Deriving the phase/amplitude ODEs

**Phase/Amplitude Approach:** This approach looks for a solution of variable phase and amplitude

$$y(x) = A(x)e^{i\Phi(x)}$$

Now differentiating twice gives

$$y''(x) = [A'' + 2iA'\Phi' + iA\Phi'' - \Phi'^2 A] e^{i\Phi(x)}$$

Setting  $m = \Phi'(x)$ , and separating the real and imaginary parts, the Shrödinger equation (1) becomes

$$\begin{aligned} A'' + [V - \lambda - m^2] A &= 0 \\ 2A'm + Am' &= 0 \end{aligned}$$

The second equation (imaginary part) has the solution

$$A = \frac{A_0}{\sqrt{m}} \quad (1.1)$$

where  $A_0$  is an arbitrary constant, without loss of generality we can set  $A_0 = 1$ . This allows for the elimination of  $A$  or  $m$  in the real part of the Schrödinger equation. Eliminating  $m$  gives

$$A'' + [V - \lambda]A = \frac{1}{A^3} \quad (1.2)$$

Milnes equation. Eliminating  $A$  yields

$$m'' - \frac{3m'^2}{2m} + 2[m^2 + \lambda - V]m = 0 \quad (1.3)$$

Notice that in making this change of variable we have moved from having a linear ODE (1) to a nonlinear ODE, and in the process increased the number of boundary conditions required to obtain a unique solution. These equations remain to be solved to generate the general solution to equation (1) noting that for real solutions

$$y(x) = Y_0 A \sin \left( \int_{x_0}^x A^{-2}(x') dx' + \Phi_0 \right) \quad (1.4)$$

$$y(x) = Y_0 \frac{1}{\sqrt{m}} \sin \left( \int_{x_0}^x m(x') dx' + \Phi_0 \right) \quad (1.5)$$

where  $Y_0$  and  $\Phi_0$  are arbitrary constants.

**The Milne Approach:** In the note by Milne [11] the general solution is recovered with variable phase and amplitude by first noting that equation (1) on the interval  $-\infty < x < \infty$  has two particular independent solutions  $y_1(x)$  and  $y_2(x)$  satisfying

$$\begin{aligned} y_1(x_0) &= 1, & y_2(x_0) &= 0, \\ y_1'(x_0) &= 0, & y_2'(x_0) &= a \neq 0 \end{aligned}$$

for some  $x_0$  in the interval and a constant arbitrary  $a$ . The Wronskian, a result from classical ODE theory is an invariant of this problem hence (pages 189-191 [14])

$$y_1(x)y_2'(x) - y_2(x)y_1'(x) \equiv a \quad (1.6)$$

Defining  $w(x)$  as

$$w(x) = [y_1^2(x) + y_2^2(x)]^{1/2}$$

, differentiating twice and eliminating  $y_1''(x)$  and  $y_2''(x)$  using equation (1) and simplifying by using equation (1.6) we obtain the so called ‘‘Milne’s equation’’

$$\frac{d^2w}{dx^2} + [V(x) - \lambda]w = \frac{a^2}{w^3}$$

Note that this is analogous to equation (1.2) if  $a = 1$  so that the function  $w$  and the amplitude  $A$  coincide in this case (alternatively make the transformation  $w(x) \rightarrow a^{1/2}w(x)$ ). The general solution of the time independent Schrödinger equation is then

$$y(x) = Y_0 w(x) \sin \left\{ a \int_{x_0}^x w^{-2}(x') dx' - \Phi_0 \right\} \quad (1.7)$$

where  $Y_0$ ,  $a$  and  $\Phi_0$  are arbitrary constants (this can be seen by substituting into Milne’s equation to recover the Schrödinger equation). Note a cosine yields an equally valid solution corresponding to  $\Phi_0 \rightarrow \Phi_0 - \pi/2$

## 1.2 Solving the phase/amplitude ODEs

Having derived the phase/amplitude ODEs, namely equations (1.2) and (1.3) we now discuss the method of their solving. The scheme employed is the classic fourth order Runge-Kutta scheme which is widely employed in solving ODEs as it provides a good compromise between accuracy and computational expense.

The region is discretised into  $N$  intervals  $dx$  in length where the region is  $[x_0, X]$ ,  $X = Ndx$ . As mentioned in the introduction the actual interval of interest is  $[x_0, \infty)$  so  $X$  is chosen far enough past the turning point of the potential such that the decaying behaviour in applying the boundary condition  $y \rightarrow 0$  as  $x \rightarrow \infty$  is as accurate as possible. Equation (1.2) or (1.3) are expressed as a system of first order ODE's with the additional ODE for  $\Phi$  the phase, for example

$$\Phi(x) = \int_{x_0}^x A^{-2}(x') dx'$$

so

$$\Phi'(x) = A^{-2}(x)$$

Thus the system to solve is for amplitude (equation (1.2))

$$\begin{aligned} A_1'(x) &= A_2(x) \\ A_2'(x) &= \frac{1}{A_1^3(x)} - (V(x) - \lambda) A_1(x) \\ \Phi'(x) &= \frac{1}{A_1^2(x)} \end{aligned} \tag{1.8}$$

or for phase (equation (1.3))

$$\begin{aligned} m_1'(x) &= m_2(x) \\ m_2'(x) &= \frac{3m_2^2(x)}{m_1^2(x)} - 2(m_1^2(x) - V(x) + \lambda) m_1(x) \\ \Phi'(x) &= m_1(x) \end{aligned} \tag{1.9}$$

Given initial conditions, from section 1.3.1, we integrate one of these systems over the interval  $[x_0, X]$  with the treatment of the boundary condition at  $X$  is discussed in section 1.3.2. The fourth order Runge-Kutta (RK4) scheme is a non-linear single step method where solving an initial value problem of the form  $y' = f(x, y)$  follows from the initial condition via

$$y_{n+1} = y_n + \frac{dx}{6} (k_1 + 2k_2 + 2k_3 + k_4)$$

where  $y_n = y(ndx)$ ,  $n$  is the step, and the  $k$ 's are given by

$$\begin{aligned} k_1 &= f(ndx, y_n) \\ k_2 &= f\left(ndx + \frac{dx}{2}, y_n + \frac{dx}{2}k_1\right) \\ k_3 &= f\left(ndx + \frac{dx}{2}, y_n + \frac{dx}{2}k_2\right) \\ k_4 &= f(ndx + dx, y_n + dxk_3) \end{aligned}$$

## 1.3 Boundary Conditions

Now that we have discussed the equations and the method of their solution, we must now consider the boundary conditions and their application. It has already been mentioned that the non-uniqueness of the phase and amplitude in the phase/amplitude solution leads to the requirement of extra boundary conditions. The arbitrary constant,  $Y_0$ , in equations (1.5) and (1.4) mean that the amplitude is arbitrary to a multiplicative constant, this means in a sense we have some freedom in the choice of the boundary conditions at the start of the interval, which we will refer to as the initial conditions.

### 1.3.1 Initial Conditions

Having set up our solver as an initial value problem, we have to supply 'initial conditions'; the boundary conditions at the beginning of the region we are solving over.

In terms of the full solution the initial conditions refer to

$$y(x_0) = \frac{Y_0}{\sqrt{m(x_0)}} \sin \Phi_0$$

so this implies the conditions on  $\Phi_0$  for non-trivial solutions

$$\begin{aligned}
y(x_0) = 0 &\Rightarrow \Phi_0 = 0 \\
y(x_0) \neq 0 &\Rightarrow \Phi_0 \neq 0
\end{aligned}$$

In cases where we have a potential symmetric about  $x_0$ ,  $\Phi_0$  is then either zero or  $\pi/2$ . It is the presence of  $Y_0$  which makes the choice of  $m(x_0)$  or  $A(x_0)$  arbitrary. In general, most boundary conditions will lead to an oscillatory behaviour of  $A$  and  $\Phi$ . However, there exist boundary conditions which yield monotonically increasing  $A$  and  $\Phi$ , more in agreement with our physical expectations of how a varying phase and amplitude should behave. One possible way to obtain this behaviour is to use a WKB approximation for specifying  $A$  and  $\Phi$  at  $x_0$ .

The WKB approximation assumes the variables are slowly varying with respect to  $x$ . i.e. let  $x = \epsilon\chi$  where  $\epsilon$  is some small parameter. This results in our neglecting terms involving derivatives with respect to  $x$  since, for example

$$\frac{dm}{dx} = \epsilon \frac{dm}{d\chi}$$

This technique is well known to produce smooth continuous solutions [9], where oscillations are damped from the solution of  $A$  and  $\Phi$ . Now our system of first order ODE's that we are solving are, if we solve for amplitude from equation (1.2), given by equations (1.8). Taking the WKB approximation the initial conditions will be

$$\begin{aligned}
A_1(x_0) &= \frac{1}{(V(x_0) - \lambda)^{1/4}} \\
A_2(x_0) = A_1'(x_0) &= -\frac{V'(x_0)}{4(V(x_0) - \lambda)^{5/4}} \\
\Phi(x_0) &= 0
\end{aligned} \tag{1.10}$$

Similarly for equations (1.9) the WKB initial conditions are simply

$$\begin{aligned}
m_1(x_0) &= (V(x_0) - \lambda)^{1/2} \\
m_2(x_0) &= \frac{V'(x_0)}{2(V(x_0) - \lambda)^{1/2}} \\
\Phi(x_0) &= 0
\end{aligned}$$

Notice these conditions require that  $V(x_0) \neq \lambda$ .

It is important to note that other initial conditions can be chosen, with varying degrees of smoothness of solution. Another method to reduce any oscillations in the phase and amplitude would be to employ a calculus of variations type argument to minimise the length of the phase or amplitude curves. We will in due course investigate the validity of choosing these initial conditions and demonstrate the oscillations that this approach damps out.

### 1.3.2 Boundary Condition at infinity

To obtain a unique solution to equations (1.8) or (1.9) we must now consider how to treat the boundary condition at the end of the interval we are considering, corresponding to the behaviour we seek at infinity. The problem posed still requires the computation of the eigenvalue  $\lambda$  and it is in the application of the boundary condition at infinity that we can impose a condition on  $\lambda$ . Note that phase and amplitude are both dependent upon the eigenvalue as well as position. At infinity we set

$$\lim_{x \rightarrow +\infty} \int_{x_0}^x m(x'; \lambda) dx' + \Phi_0 = k\pi \tag{1.11}$$

assuming we express the full solution in terms of sine. Crucially this boundary condition means that we are restricting the behaviour past the turning point to that of decay as we seek a method to converge upon the above condition at the end point of the interval.

For large  $x$  we can write

$$\Phi(x) = \int_{x_0}^x m(x'; \lambda) dx' = k\pi + \int_x^{+\infty} m(x'; \lambda) dx'$$

where  $R = \int_x^{+\infty} m(x'; \lambda) dx'$  is the ‘Residual’. Thus, assuming  $\Phi_0 = 0$

$$\sin \left\{ \int_{x_0}^x m(x'; \lambda) dx' \right\} = \sin(k\pi + R) = \sin R \approx R$$

for small  $R$ . This implies that when  $y$  becomes small we can examine the behaviour by making the approximation locally

$$y(x) \approx \frac{Y_0}{\sqrt{-R'(x)}} R(x) \tag{1.12}$$

since  $m(x) = -R'(x)$  from the definition.

The result in terms of the numerical method used here is that we attempt to make  $\Phi(X) = k\pi$  at some finite point  $X$  from the turning point of the potential. Thus by some iterative procedure, or shooting method, we attempt to set the residual  $R(X) = 0$ . One advantage of this method is that choosing the form of the boundary condition in this way, isolates the ‘eigenmode’ by appropriate selection of  $k$  and thus the shooting method has an easier task to converge upon the eigenvalue.

## 1.4 Shooting Method

Having prescribed a condition on  $\lambda$  via the boundary condition, it then must be discussed how the iterative process converges upon the eigenvalue and boundary condition.

The shooting method involves solving the ODE’s by the RK4 method described (or an alternative solver) with the appropriate initial conditions at the start of the interval for each value of  $\lambda$  and obtaining the discrepancy in the boundary condition at the end of the interval; the residual. The new  $\lambda$  is then computed such that this discrepancy is reduced on solving the ODEs in the next iteration. The method for updating  $\lambda$  can be a bisection method,

or a Newton-Raphson solver or a combination thereof <sup>1</sup>. Traditionally the shooting method for solving boundary value problems involves iterating on the derivative initial condition to converge on the end boundary condition.

In general for the phase/amplitude method we employ Newton-Raphson iteration to converge on the eigenvalue  $\lambda$ , since by isolating the eigenmode with the boundary condition we eliminate the need for a close first guess on  $\lambda$ . We update  $\lambda$  for successive iterations by means of

$$\lambda_{new} = \lambda_{old} - \frac{R_X}{dR_X/d\lambda}$$

where  $X$  is the end of the region we are solving over thus  $R_X$  is the residual at  $X$ .

$$R_X = \int_{x_0}^X m(x'; \lambda) dx' - k\pi$$

Hence in the routine we have an iteration loop, on each pass solving the phase/amplitude ODE using the RK4 procedure with a new eigenvalue until the boundary condition is satisfied (see figure 1.1). We thus have a stopping criterion on the iteration loop that  $y(X) < \epsilon$  where  $\epsilon$  is some small parameter. Note that the iteration uses the residual of the phase in the convergence of  $\lambda$  though the stopping criterion is not that the residual should tend to zero but that the final solution should. This is important since as the residual goes to zero, the amplitude tends to infinity (equation (1.12)). It was found that too small an  $\epsilon$  would hamper convergence since the eigenvalues will converge at machine precision (double) before the residual has met the convergence criterion and thus no further iterations are possible. Careful analysis found that an optimum value was  $\epsilon \approx 10^{-8}$ .

The iteration loop was bounded such that if it proceeded through 20 iterations, the method was deemed not to have converged to prevent the routine becoming stuck in an infinite loop.

From Korsch and Laurent (1981) [9] and earlier Yuan et. al. (1974) [16] we can derive an expression for  $dR_X/d\lambda$  provided  $A'(x_0) = 0$  (i.e. that

---

<sup>1</sup>See [4] Section 3.1-3.3 & 8.8 and [3] Section 2.3 & 11.2

$V(x_0) = 0$ . If this condition is not satisfied we use a finite difference, see later). Starting from the following equations

$$\begin{aligned}\frac{\partial}{\partial x} \left[ y \frac{dy'}{d\lambda} \right] &= y \frac{\partial y''}{\partial \lambda} + y' \frac{\partial y'}{\partial \lambda} \\ \frac{\partial}{\partial x} \left[ y' \frac{dy}{d\lambda} \right] &= y'' \frac{\partial y}{\partial \lambda} + y' \frac{\partial y'}{\partial \lambda}\end{aligned}$$

where primes denote derivatives with respect to  $x$ . Now using these expressions and equation (1)

$$\frac{\partial}{\partial x} \left[ y' \frac{dy}{d\lambda} - y \frac{dy'}{d\lambda} \right] = y^2 \frac{\partial (V(x) - \lambda)}{\partial \lambda} = -y^2 \quad (1.13)$$

Using the phase amplitude solution

$$y(x) = Y_0 A(x) \sin \left\{ \int_{x_0}^x A^{-2}(x') dx' - \Phi_0 \right\}$$

and without loss of generality set  $Y_0 = 1$ , then

$$\begin{aligned}y' \frac{dy}{d\lambda} - y \frac{dy'}{d\lambda} &= \left\{ A' \frac{\partial A}{\partial \lambda} - A \frac{\partial A'}{\partial \lambda} \right\} \sin^2(\Phi(x) - \Phi_0) \\ &\quad + \cos^2(\Phi(x) - \Phi_0) \frac{\partial(\Phi(x) - \Phi_0)}{\partial \lambda} \\ &\quad + \sin^2(\Phi(x) - \Phi_0) \frac{\partial(\Phi(x) - \Phi_0)}{\partial \lambda} \\ &\quad - A^2 \cos(\Phi(x) - \Phi_0) \sin(\Phi(x) - \Phi_0) \frac{\partial A^{-2}}{\partial \lambda} \\ &= \left\{ A' \frac{\partial A}{\partial \lambda} - A \frac{\partial A'}{\partial \lambda} \right\} \sin^2(\Phi(x) - \Phi_0) + \frac{\partial(\Phi(x) - \Phi_0)}{\partial \lambda} \\ &\quad - A^2 \frac{\sin 2(\Phi(x) - \Phi_0)}{2} \frac{\partial A^{-2}}{\partial \lambda}\end{aligned}$$

Now integrating equation (1.13) from  $x_0$  to  $X$ , setting  $\Phi_0 = \Phi(X)$  since  $\Phi_0$  is arbitrary and noting that we have made the assumption that we use the initial conditions laid out in section 1.3.1 and that  $V(x_0) = 0$  we have

$$\frac{\partial \Phi(X)}{\partial \lambda} = \int_{x_0}^X A^2(x') \sin^2 [\Phi(x') - \Phi(X)] dx' + A^2(x_0) \frac{\partial A^{-2}(x_0)}{\partial \lambda} \frac{\sin 2\Phi(x)}{2}$$

Now applying the initial conditions we obtain

$$\frac{dR_X}{d\lambda} = \frac{\partial\Phi(X)}{\partial\lambda} = \int_0^X A^2(x') \sin^2(\Phi(x') - \Phi(X)) dx' + \frac{\sin(2\Phi(X))}{4\lambda} \quad (1.14)$$

It was found to be sufficient for this integral to be calculated using a simple composite trapezoidal rule (pages 516-517 [4]) namely

$$\int_0^X f(x') dx' = dx \left( \frac{f(0)}{2} + \sum_{i=1}^{N-1} f(idx) + \frac{f(N)}{2} \right)$$

where  $dx$  is the step size and here

$$f(x) = A^2(x) \sin^2(\Phi(x) - \Phi(X))$$

We can then use equation (1.14) to converge upon a value for  $\lambda$  for which the solution satisfies the boundary conditions.

An alternative to this form of Newton iteration, where it is not possible to make the above calculation, is to use a backward finite difference for the derivative of the residual, i.e.

$$\lambda_{i+1} = \lambda_i - \frac{R(\lambda_i)(\lambda_i - \lambda_{i-1})}{R(\lambda_i) - R(\lambda_{i-1})}. \quad (1.15)$$

where  $i$  denotes the current iteration step. This is known as the secant method and is useful where no expression for  $dR_X/d\lambda$  can be found. Notice, however, that this form requires two starting values in the numerical technique and is a less accurate approximation of  $dR_X/d\lambda$  and as such does not allow as rapid a convergence as the explicit expression for  $dR_X/d\lambda$ . The Secant Method's convergence is superlinear, as opposed to standard Newton method whose convergence is quadratic. The benefit is, however, that fewer function evaluations are required; Newton requires  $R_X$  and  $dR_X/d\lambda$  where Secant only requires  $R_X$  (see [4] pages 102-104 for further details). The Secant method, as with Newton, in general is reliant on a good first guess at  $\lambda$ .

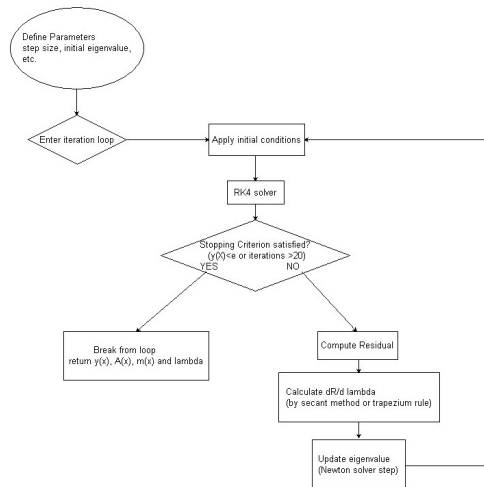


Figure 1.1: A Flow chart showing the steps in the phase amplitude routine.

## 1.5 MATLAB routine

Figure 1.1 is a flow chart outlining the stages involved in the phase/amplitude method routine. This was programmed in MATLAB and the code can be found in the appendix along with instructions on its use.

To allow objective assessment of the analysis which follow, it is important that we note machine precision. In MATLAB this is given by  $\text{eps} = 2^{-52} = 2.22e - 016$  and is defined as the distance from 1.0 to the next floating point number.

## 1.6 Alternative Numerical Methods

In order for this study to make good comparisons and conclusions about the accuracy and efficiency of the phase/amplitude method it is necessary to consider other numerical techniques in use in the solution of the Schrödinger equation (1).



have  $y'(x_0) = 0$  we make  $y_{-1} = y_1$ . Thus in our  $A$  matrix we have an extra row for  $y_0$  in which we impose this condition, resulting in the second entry being double since

$$\begin{aligned} \frac{y_{-1} - 2y_0 + y_1}{dx^2} + (V_0 - \lambda)y_0 &= 0 \\ \Rightarrow \frac{-2y_0 + 2y_1}{dx^2} + (V_0 - \lambda)y_0 &= 0 \end{aligned}$$

We can then employ the routines in MATLAB (`eig`) to compute the eigenvalues and solutions, note that such methods calculate  $N$  eigenvalues and eigenvectors which for high resolutions is quite computationally expensive. The task is, however made easier since the matrix  $A$  is tridiagonal, and in the Dirichlet case symmetric, meaning that no reduction to that form is required within the algorithm. Such a discretisation will result in a second order accurate solution due to the second order differencing.

### 1.6.2 Direct Shooting Method

As previously mentioned it is possible to discretise our region and directly solve equation (1) using a fourth order Runge-Kutta scheme with a shooting method on  $\lambda$  to fix the far boundary condition as in the phase/amplitude method by means of an iteration loop and a tolerance on  $y(X)$ . Without a means of specifying the mode, as we do with the boundary condition in the phase/amplitude method, the task of converging on the resonant modes becomes slightly more involved. A straight forward Newton solver has the drawback of requiring a close guess to converge upon or find a specific eigenvalue over neighbouring modes. However the typical way to circumvent this problem is to begin the routine with a few iterations of a bisection method (section 3.1 [4]). This entails beginning with an interval for  $\lambda$  i.e.  $[\lambda_0, \lambda_1]$  and solving equation (1) to find the residual (in this case simply  $y(X)$ ) for each end point, and the mid point  $(\lambda_1 + \lambda_0) / 2$ . Then by examining the signs of the residues we can half the interval to contain the solution. In this way we

can begin from a broad guess (or range) for  $\lambda$  and quickly find a closer estimate from which to begin the Newton iteration. If we use our fourth order RK-4 solver, this presents a more accurate method than the standard matrix eigenvalue technique described above. In comparison with the phase/amplitude method, a standard shooting method requires a secant method (with  $y(X)$  taking the role of residual) in contrast to the straight forward Newton iteration for the phase/amplitude method which has an explicit expression for  $dR/d\lambda$  (equation (1.14) when  $V(x_0) = 0$ ).

As with the standard discretisation the form of the initial conditions is decided upon by the requirement of  $y(x_0)$  to be zero or not. If not we impose a Neumann condition since  $y(x_0)$  is unspecified by the problem. For the example of a symmetric potential, and hence solutions we would have

$$\begin{aligned} y(x_0) &= 0 \quad , \quad y'(x_0) \neq 0 \\ y(x_0) &\neq 0 \quad , \quad y'(x_0) = 0 \end{aligned}$$

This method is more common place in the meteorological literature for solving eigenvalue problems of this type.

### 1.6.3 WKB approximation

The WKB approximation was introduced to allow us to set up our initial conditions, it can, however, yield an approximation for our solution in the region before any turning point of the potential. For example

$$y(x) = (V(x) - \lambda)^{-1/4} \sin \int_{x_0}^x \sqrt{V(x) - \lambda} dx$$

This approximation is commonly used in problems of this type and is employed to give smooth phase and amplitude. The difficulty with this approximation, aside from the loss in accuracy near and past the turning point, is that it requires the prior knowledge of  $\lambda$ .

By examining particular examples of the Schrödinger equation in a meteorological context it is the intention of the following chapters to test the

phase/amplitude method against known analytic solutions and the alternative methods outlined above, in accuracy, speed of convergence and resolution effects to validate its use in the study of such waves. It is also the intention of the author to provide some commentary of the findings, results and the wave motions themselves to provide a more thorough analysis of this methods worth.

# Chapter 2

## Equatorial Waves

The use of the Schrödinger equation in the study of trapped equatorial inertio-gravity <sup>1</sup>, Kelvin and Rossby waves was first introduced by Matsuno (1966) [10] and later included in several texts concerned with the dynamics of the atmosphere and oceans (Gill [7], Holton [8]). The important feature at the equator is the vanishing of the Coriolis force, thus restricting geostrophic motions to higher latitudes. Matsuno's work involved a linearised shallow water equation model on a Cartesian coordinate system with a constant  $\beta$ -plane approximation (The Coriolis parameter is assumed proportional to latitude  $f = \beta y$ ).

### 2.1 $\beta$ -plane Derivation

Our equation set in this regime is

$$\begin{aligned}\frac{\partial u}{\partial t} - \beta y v + \frac{\partial \phi}{\partial x} &= 0 \\ \frac{\partial v}{\partial t} + \beta y u + \frac{\partial \phi}{\partial y} &= 0 \\ \frac{\partial \phi}{\partial t} + gH \left( \frac{\partial u}{\partial x} + \frac{\partial v}{\partial y} \right) &= 0\end{aligned}$$

---

<sup>1</sup>An inertio-gravity wave is simply a gravity wave of time and length scales sufficiently large as to allow the earth's rotation to effect their motions.

where  $(u, v)$  is the velocity vector,  $x$  denotes the longitudinal direction,  $y$  the meridional ( $y = 0$  denoting the equator),  $\phi = gH$  is geopotential height,  $H$  the depth of the fluid layer,  $g$  the gravitational constant and  $\beta = \frac{2\Omega}{a} = 2.3 \times 10^{-11} m^{-1} s^{-1}$  the  $\beta$  parameter at the equator, where  $a$  is the earth's radius and  $\Omega$  the rotation rate..

Now we consider solutions of the form  $e^{i(kx - \omega t)}$ , that is wave solutions propagating zonally around the equator where  $k$  is a zonal wave number and  $\omega$  angular frequency. i.e.

$$(u, v, \phi) = (\hat{u}(y), \hat{v}(y), \hat{\phi}(y))e^{i(kx - \omega t)}$$

with  $\hat{u}, \hat{v}, \hat{\phi}$  being  $y$ -dependent amplitudes. With these expressions our equation set becomes

$$-i\omega\hat{u} - \beta y\hat{v} + ik\hat{\phi} = 0 \quad (2.1)$$

$$-i\omega\hat{v} + \beta y\hat{u} + \frac{d\hat{\phi}}{dy} = 0 \quad (2.2)$$

$$-i\omega\hat{\phi} + gH \left( ik\hat{u} + \frac{d\hat{v}}{dy} \right) = 0 \quad (2.3)$$

We now seek to eliminate  $\hat{u}$  and  $\hat{\phi}$  to obtain an expression for  $\hat{v}$ . Substituting  $\hat{u}$  from equation (2.1) into equation (2.3)

$$-i\omega\hat{\phi} + gH \left( \frac{ik^2}{\omega}\hat{\phi} - \frac{\beta k}{\omega}y\hat{v} + \frac{d\hat{v}}{dy} \right) = 0$$

Now differentiate and substitute for  $\frac{d\hat{\phi}}{dy}$  from equation (2.2)

$$\begin{aligned} \left( i\omega - gH\frac{ik^2}{\omega} \right) \beta y\hat{u} - gH\beta\frac{k}{\omega}y\frac{d\hat{v}}{dy} + \\ \left( \omega^2 - gHk^2 - gH\beta\frac{k}{\omega} \right) \hat{v} + gH\frac{d^2\hat{v}}{dy^2} = 0 \end{aligned} \quad (2.4)$$

Now substituting  $\hat{\phi}$  from equation (2.1) into equation (2.3) gives

$$-i\frac{\omega^2}{k}\hat{u} - \frac{\omega}{k}\beta y\hat{v} + gH\left(ik\hat{u} + \frac{d\hat{v}}{dy}\right) = 0 \quad (2.5)$$

which we can use to eliminate  $\hat{u}$  in equation (2.4) to give us

$$\frac{d^2\hat{v}}{dy^2} + \left(\frac{\omega^2}{gH} - k^2 - \beta\frac{k}{\omega} - \frac{\beta^2 y^2}{gH}\right)\hat{v} = 0 \quad (2.6)$$

the time independent Schrödinger equation.

## 2.2 Analytic Solutions

Equation (2.6) can be recast into non-dimensional form via the following transformation to enable us to apply known analytic solutions for equations of this form (Holton [8]).

$$\tilde{y} = \left(\frac{\beta}{\sqrt{gH}}\right)^{1/2} y$$

Thus equation (2.6) becomes

$$\frac{d^2\hat{v}}{d\tilde{y}^2} + \left(\frac{\sqrt{gH}}{\beta}\left(\frac{\omega^2}{gH} - k^2 - \beta\frac{k}{\omega}\right) - \tilde{y}^2\right)\hat{v} = 0$$

For a classical Schrödinger equation with parabolic potential of the form

$$\frac{d^2Y}{dX^2} + (\lambda - X^2)Y = 0$$

solutions are well known in the form of parabolic cylinder functions (Abramowitz and Stegun [1] and Bateman [2]).

The classical result for eigenmodes decaying at infinity ( $Y \rightarrow 0$  as  $X \rightarrow \infty$ ) is that the eigenvalues take on the odd integers:

$$\lambda = 2n + 1 \quad (n = 0, 1, 2, \dots)$$

The parabolic cylinder functions in this case are given by

$$\hat{Y}(X) = Y_0 H_n(X) e^{-X^2/2} \quad n = 0, 1, 2, \dots \quad (2.7)$$

where  $H_n(X)$  denotes the  $n$ th Hermite Polynomial, the first few being

$$H_0 = 1, \quad H_1(X) = 2X, \quad H_2(X) = 4X^2 - 2$$

and obeying the recurrence relation

$$H_{n+1} = 2XH_n(X) - 2nH_{n-1}(X)$$

Thus in the case of the trapped equatorial waves, the following relation follows [10]

$$\frac{\sqrt{gH}}{\beta} \left( \frac{\omega^2}{gH} - k^2 - \beta \frac{k}{\omega} \right) = 2n + 1 \quad (n = 0, 1, 2, \dots) \quad (2.8)$$

thus equation (2.6) becomes

$$\frac{d^2 \hat{v}}{d\tilde{y}^2} + (2n + 1 - \tilde{y}^2) \hat{v} = 0 \quad (2.9)$$

And the parabolic cylinder functions are similarly

$$\hat{v}(\tilde{y}) = v_0 H_n(\tilde{y}) e^{-\tilde{y}^2/2} \quad n = 0, 1, 2, \dots \quad (2.10)$$

Figure 2.1 shows the first three solutions. Notice that even  $n$  recover even solutions and odd  $n$  the odd solutions.

## 2.3 Numerical Solutions

These analytic solutions provide a useful means of testing and validating our phase/amplitude method and comparing it against the alternative numerical techniques. The numerical results presented will be solutions of the non-dimensional equation (2.9) and as such we will have in general the dispersion relation

$$\lambda = \frac{\sqrt{gH}}{\beta} \left( \frac{\omega^2}{gH} - k^2 - \beta \frac{k}{\omega} \right) = 2n + 1 \quad (2.11)$$

as eigenvalue and potential  $V(x) = -\tilde{y}^2$ .

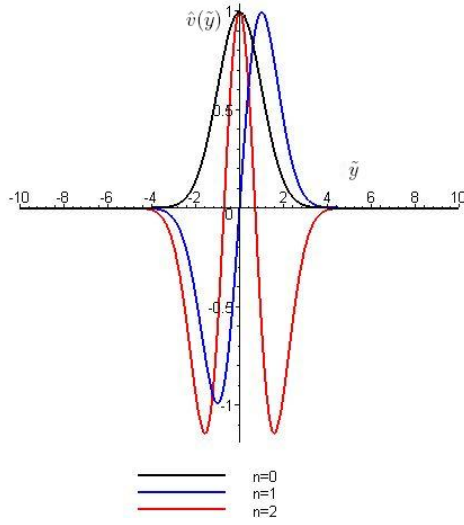


Figure 2.1: Exact Solution of equation (2.2) in terms of Hermite Polynomial solutions in Non-dimensional coordinates.

Mode $n$	Phase/Amplitude	Std Shooting	Matrix Eigenvalue
0	1.8e-009	2.7e-010	-0.011
1	4.0e-009	1.6e-009	3.1e-005
2	3.3e-009	6.8e-009	-0.028
3	6.6e-009	1.8e-008	1.6e-004
4	4.1e-009	3.8e-008	-0.038

Table 2.1: Accuracy of computed eigenvalues for the various methods  $|2n + 1 - \lambda|$ . Integration length  $X = 7$ , step size  $dy = 0.01$ .

Mode $n$	Phase/Amplitude	Std Shooting	Matrix Eigenvalue
0	1.6e-005	1.0e-006	0.12
1	3.3e-005	1.5e-005	3.1e-003
2	2.4e-005	6.6e-005	0.28
3	5.4e-005	1.8e-004	1.5e-002
4	2.8e-005	3.7e-004	0.36

Table 2.2: Accuracy of computed eigenvalues for the various methods  $|2n + 1 - \lambda|$ . Integration length  $X = 7$ , step size  $dy = 0.1$ .

### 2.3.1 Accuracy of $\lambda$ & Resolution

Tables 2.1 and 2.2 show the accuracy of  $\lambda$  for the three methods under consideration namely the phase/amplitude method, the direct shooting method and the BVP matrix eigenvalue method for step size  $dx = 0.01$  and  $dx = 0.1$  respectively. The interval was chosen to be  $[0, 7]$  such that we integrate in both directions about the equator. Notice however that the solutions are symmetric/antisymmetric about the equator, thus it is really only necessary to integrate in one direction. This interval also encompasses the interesting behaviour of the first 5 modes, as it is far enough past the turning points to ensure we include the decaying behaviour. The step sizes are chosen as a compromise between accuracy and computational expense. Recovering the odd modes (odd  $n$ ) relies on setting  $\Phi_0 = \pi/2$ , as described in discussing a symmetric potential.

The results indicate that the phase/amplitude method is more consistently accurate on increasing  $n$  compared to the standard shooting method. The error is expected to increase with increasing  $n$  as the number of oscillations in the solution increase, this effect seems to be less evident with the phase/amplitude method. It is not clear on first impression that it is in evidence at all, however if we notice the distinction between odd and even solutions, they follow the trend independently of each other while remaining comparable in order of magnitude. Interestingly the standard shooting method is the method of choice for the lowest values of  $n$ , however as  $n$  increases the error also increases significantly.

The phase/amplitude method and standard shooting method both use a fourth order solver and this is borne out in comparing the error between the step sizes, four orders of magnitude are lost in error by a single order of magnitude reduction in step size.

The matrix method does not show easy comparisons. Firstly there is a considerable difference between the odd and even solutions. This can only be attributed to the treatment of the boundary condition, where Dirichlet data recovers the odd solutions and Nuemann the even. This is also the same

treatment used in the standard shooting method, but clearly accuracy is compromised by approximating this boundary data via a second order finite difference as described in section 1.6. Thus we see the odd solutions being more accurate and conforming to the second order accuracy with the change in step size. The even solutions are far less accurate and are also not second order accurate.

### 2.3.2 Convergence

Mode $n$	Phase/Amplitude Iterations (Newton)	Phase/Amplitude Iterations (secant)	Std Shooting Iterations
0	9	10	11
1	6	7	11
2	5	7	11
3	5	7	11
4	5	7	11

Table 2.3: Number of iterations for convergence for the phase/amplitude for Newton and secant solvers and shooting method (including bisection iterations).  $X$  integration length as in table 2.1 with  $dy = 0.01$ .

Table 2.3 shows the number of iterations required for convergence of the two ‘shooting’ type methods. The phase/amplitude method is an improvement in this respect, converging with fewer iterations compared to the standard shooting method. The Newton iteration using equation (1.14) improves the method further over the secant method, equation (1.15) as expected. It was also noticed during the course of these tests that a change in the resolution had no effect on the number of iterations required for convergence and also that using the secant or Newton iteration in the phase amplitude method had no impact on its accuracy. As with accuracy it seems that the phase/amplitude method is not so efficient at the lower modes, especially  $n = 0$ . This may be in part due to integrating far past the turning point in

this case, since the interval for the tests was  $[0, 7]$  for all modes. Reducing this to  $[0, 5]$  for  $n = 0$  reduced the required iterations to 8, while the accuracy remained as in table 2.1. It is interesting that the standard shooting method shows no distinction between the modes in terms of iterations needed for convergence.

The stopping criterion in general are tighter for the phase/amplitude method, despite the fewer iterations it takes for accurate convergence. The choices for the stopping criterion, based upon the error in the full solution as  $x \rightarrow X$  is explored in more depth in the following section.

The phase amplitude method, in the test carried out here had an initial guess of  $\lambda_0 = 10$  for each eigenmode with the boundary condition (1.11) being the mechanism for selecting between them.

The method for converging on the full set of resonant modes for the standard shooting method is in part from the initial conditions (distinguishing between odd/even eigenmodes) and then by systematic choices for the initial given interval for  $\lambda$  (for which the bisection iterations give the starting secant iteration value for convergence to the eigenvalue). This requires slightly more user input and more complex algorithm than the phase/amplitude method and it is the author's opinion that the phase/amplitude method presents a far more elegant and efficient way to recover the eigenmodes via selecting  $k$  in the boundary condition.

### 2.3.3 Error in full Solution

Having computed the resonant modes, it is possible to compute the full solution of  $\hat{v}(\tilde{y})$  from the numerical calculations to compare against the parabolic cylinder functions. Since we are dealing with non-dimensional solutions and the phase/amplitude solution is non-unique to a multiplicative constant, the solutions are normalised to provide a comparison.

Figure 2.2 shows the errors of the normalised solution of  $\hat{v}(\tilde{y})$  for various wave modes. It is evident that increasing  $n$  leads the phase/amplitude method to be comparatively more accurate, as noted with the eigenvalue

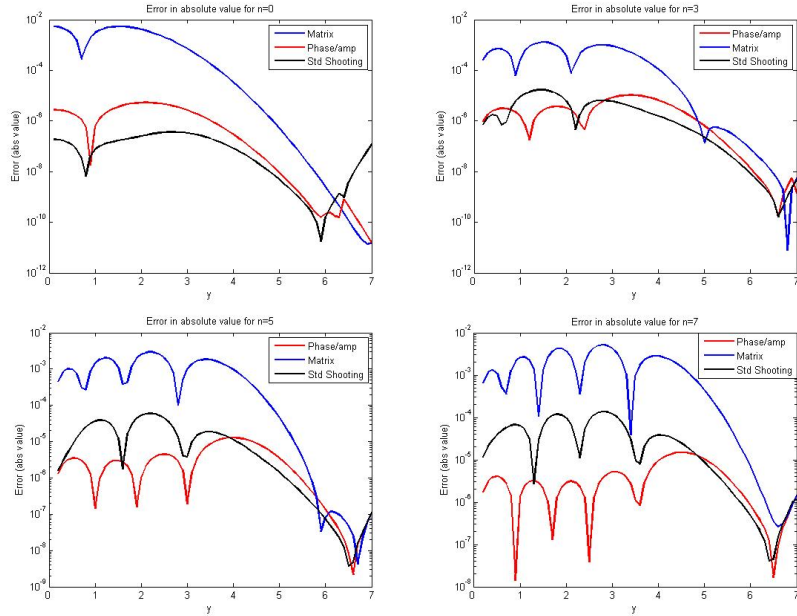


Figure 2.2: Error in absolute values of  $\hat{v}$  of the numerical methods under consideration, compared to analytic solution (equation (2.10) for various  $n$  with non-dimensional  $y = \tilde{y}$ .  $dy = 0.1$  (Logarithmic axis)

computations.

Table 2.4 shows the error in the computed solution for  $\hat{v}(\tilde{y})$  under the  $L_2$  norm. This is calculated by

$$\|y_e - y_n\|_{L_2} = \int_0^X (y_e - y_n)^2 dx'$$

where  $y_e$  and  $y_n$  represent the analytic and numerical solutions respectively. This was computed using the composite trapezoidal rule as described in the first chapter. The error in the full solution was found to be quite sensitive to the stopping criterion. This is highlighted by the error for the  $n = 0$  mode. From the plots in figure 2.2 and the error in the computed eigenvalue it appears that the standard shooting method is the more accurate method. However the  $L_2$  norms suggest the phase/amplitude method to be more accurate. This is due to the phase/amplitude method being more accurate towards the end of the interval where  $x \rightarrow X$  since it allows for a tighter

Mode $n$	Phase/Amplitude	Std Shooting	Matrix Eigenvalue
0	1.8e-019	1.7e-017	4.0e-008
1	1.8e-018	1.6e-018	1.7e-012
2	5.3e-019	1.4e-018	1.2e-007
3	8.0e-019	2.6e-019	2.0e-011
4	2.3e-018	3.0e-018	2.1e-007

Table 2.4: Accuracy of computed solutions in terms of  $L_2$  norm.

stopping criterion compared to the standard shooting method ( $\epsilon 10^{-9}$  compared to  $\epsilon 10^{-6}$ ). Notice this is not the case for every mode as the turning point for each mode becomes closer to the end of the interval. The stopping criterion was fully explored in this and the previous section and values settled upon to allow accurate convergence. Smaller  $\epsilon$ , particularly in the standard shooting method, will prevent convergence as the eigenvalues will converge before the stopping criterion is reached thus preventing further iterations.

### 2.3.4 Initial Conditions

In section 1.3.1 it was explained that the WKB choice for the initial conditions was made so that the phase and amplitude remain non-oscillatory, i.e. smooth. This means that we have more accurate computations and smooth solutions. To demonstrate the importance of this a computation was carried out with the following initial conditions as an alternative to equations (1.10)

$$\begin{aligned}
 A_1(x_0) &= 1 \\
 A_2(x_0) &= 0 \\
 \Phi(x_0) &= 0
 \end{aligned}
 \tag{2.12}$$

Figure 2.3 shows the comparison between phase and amplitude for the two initial conditions for  $n = 4$  and shows up very well the oscillations that arise from different initial conditions. It was also noticed that these initial

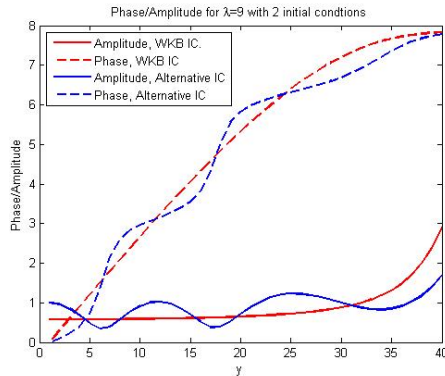


Figure 2.3: Phase and Amplitude for WKB initial conditions (equations 1.10), red, with initial conditions (2.12), blue. Non-dimensional  $y = \tilde{y}$ .  $dy = 0.1 \lambda = 9$

conditions lead to a significant loss of accuracy and an increase in the number of iterations required for convergence.

## 2.4 Wave modes

Now we have obtained solutions to equation (2.6), both analytic and numerical, we can discuss the type of motions they present.

Equation (2.11) gives us a dispersion relationship between meridional mode, frequency and wavelength (longitudinal wave number). This is in the form of a cubic in  $\omega$  and as such we will find three roots, for specified  $k$  and  $n$  ( $n \geq 1$ ), corresponding to three forms of wave motion that are permitted at the equator under this model, those being a westward and an eastward propagating inertio-gravity wave at higher frequencies and a Rossby wave typically of a lower frequency. It is possible to highlight the distinction between the wave types by making the following approximations for wave frequencies, noting that for inertio-gravity wave the term  $\omega/k$  will be small and for Rossby waves  $\omega^2$  will be small compared to the other terms. This gives the following expressions for  $\omega$  (Matsuno 1966 [10] and Gill [7])

$$\begin{aligned}
\omega_{1,2} &\approx \mp \sqrt{gH \left( k^2 + \frac{\beta}{\sqrt{gH}} (2n+1) \right)} \\
\omega_3 &\approx \frac{k}{\frac{k^2}{\beta} + \frac{2n+1}{\sqrt{gH}}}
\end{aligned} \tag{2.13}$$

where  $\omega_{1,2}$  denote the inertio-gravity wave frequencies and  $\omega_3$  the Rossby wave frequency. Now observing the phase velocities of the full dimensioned parameters

$$\begin{aligned}
c_{1g2} &\approx \mp c_g \sqrt{1 + \frac{k^2 \beta}{c_g} (2n+1)} \\
c_3 &\approx \frac{-\beta}{k^2 + \frac{\beta}{c_g} (2n+1)}
\end{aligned}$$

where  $c_g = \sqrt{gH}$  is the phase speed of pure gravity waves.

Gill [7] gave bounds on the error for these approximations. For  $n = 1$  the maximum fractional error on  $\omega$  is 13% for inertio-gravity waves and 2% for Rossby waves. Our phase/amplitude method, having proven it's accuracy in calculating  $\lambda$ , can also be adapted to obtain specific frequencies of waves given a certain wave number by shooting on  $\omega$  as opposed to  $\lambda$ . This allows us to calculate the specific frequencies for the different wave motions without the use of these approximations. This, however, presents the problem that the potential and phase are not seperable and thus the secant method described in section 1.4 needs to be employed.

Figure 2.4 is taken from Matsuno (1966) [10] and shows the allowed frequencies and wave number relationships for  $n = 0, 1, 2$ .

An interesting feature which Matsuno found was the behaviour of the waves of the  $n = 0$  mode. The westward propagating inertio-gravity wave and the Rossby wave were found not be be entirely distinct, in that the frequencies of the two wave motions overlap. This has lead to this equatorial mode being referred to as a ‘‘Rossby-gravity’’ type wave. For  $n = 0$  equation (2.11) becomes

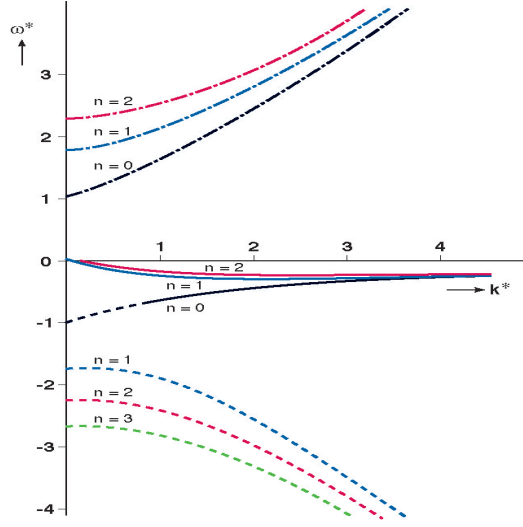


Figure 2.4: Dispersion diagram for equatorial waves with non-dimensional frequency and wave number ( $k^* = k(\sqrt{gH}/\beta)$   $\omega^* = \omega(\beta\sqrt{gH})$ ). Dashed line: westward propagating inertio-gravity waves. Solid line: Rossby waves. Chain-link line: eastward propagating inertio-gravity waves. (Matsuno 1966) [10]

$$\begin{aligned} \frac{\omega^3}{c^2} - \omega k^2 - \beta k - \frac{\beta\omega}{c} &= 0 \\ \Rightarrow \left(\frac{\omega}{c} + k\right) \left(\frac{\omega^2}{c} - k\omega - \beta\right) &= 0 \end{aligned}$$

However in using equation (2.5) to eliminate  $\hat{u}$  in the derivation of equation (2.6) we implicitly assumed that  $\frac{\omega}{c} \neq -k$ , since this would lead to a vanishing denominator in the expression for  $\hat{u}$ . Thus it would appear that the  $n = 0$  mode has only two frequencies for a specified  $k$ . This is indeed the case although we still retain the three types of wave motion as the westward wave has frequencies of Rossby waves for large  $k$  and inertio-gravity waves for small  $k$ . As such neither wave type can be distinguished from the other, leading to the notion of a mixed Rossby-gravity wave.

We can also reconstruct the full fields of  $\phi$ ,  $u$  and  $v$  from the calculated  $\hat{v}$  via

$$u = \frac{\sqrt{\beta/c}}{i(k^2 - \omega^2/c^2)} \left( \frac{\omega}{c} \tilde{y} \hat{v} - k \frac{d\hat{v}}{d\tilde{y}} \right) \exp i(kx - \omega t) \quad (2.14)$$

$$\phi = \frac{\sqrt{\beta/c}}{i(k^2 - \omega^2/c^2)} \left( \frac{ck}{\omega} \tilde{y} \hat{v} - \frac{d\hat{v}}{d\tilde{y}} \right) \exp i(kx - \omega t) \quad (2.15)$$

$$v = \hat{v} \exp i(kx - \omega t) \quad (2.16)$$

and observe from these the type of motions we expect from the waves we are considering.

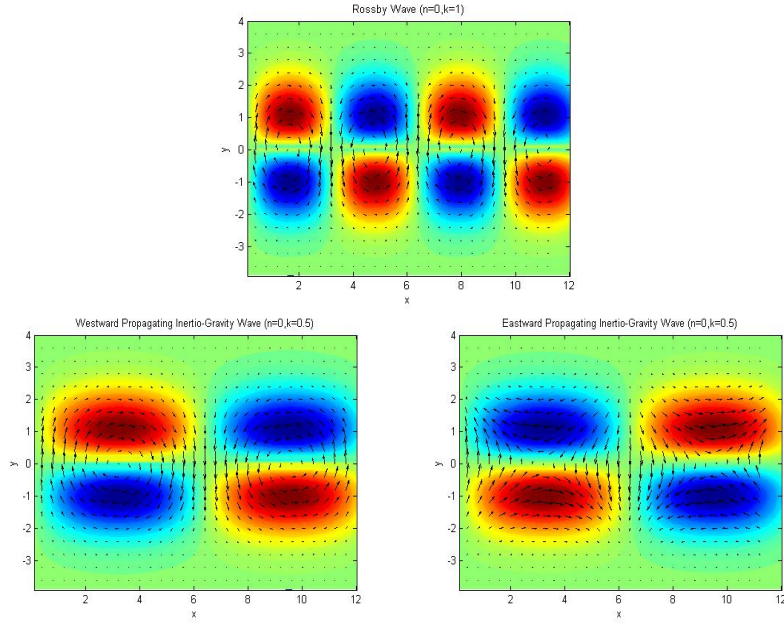


Figure 2.5: Pressure distribution (colour) and velocity vectors for  $n = 0$  mode for  $k = 0.5$  Rossby wave upper panel,  $k = 1$  westward propagating inertio-gravity wave and eastward propagating inertio-gravity wave bottom panel. Non-dimensional coordinates.

Figure 2.6 shows the geopotential height and wind vector distributions for the three wave types for  $n = 1$  and  $n = 2$ . It is expected that geostrophic motions will break down at the equator where the Coriolis force vanishes (in our  $\beta$ -plane approximation  $\beta$  is held constant and  $y$  vanishes as our coordinate system is centered on the equator). The interesting feature in figure 2.6

is that the Rossby waves of the  $n = 1$  and  $n = 2$  modes show a degree of geostrophy, shown up especially by the strong zonal winds about the equator. We also observe vortices about the equator in the  $n = 2$  case brought about by the vanishing  $f$ . The gravity waves in these cases are certainly more ageostrophic by comparison.

The more interesting case is that of  $n = 0$ . From our previous analysis of frequencies we expect for larger  $k$  Rossby wave motions to replace the westward propagating inertio-gravity wave for lower  $k$ . In fact since  $\omega$  varies continuously with  $k$  there will be no clear distinction between the motions for a given change in wavelength. Indeed in figure 2.5 we compare the westward propagating motions for  $k = 0.5$  and  $k = 1$ . They show quite similar motions, geostrophy dominating at higher latitudes, and ageostrophic motions towards the equator.

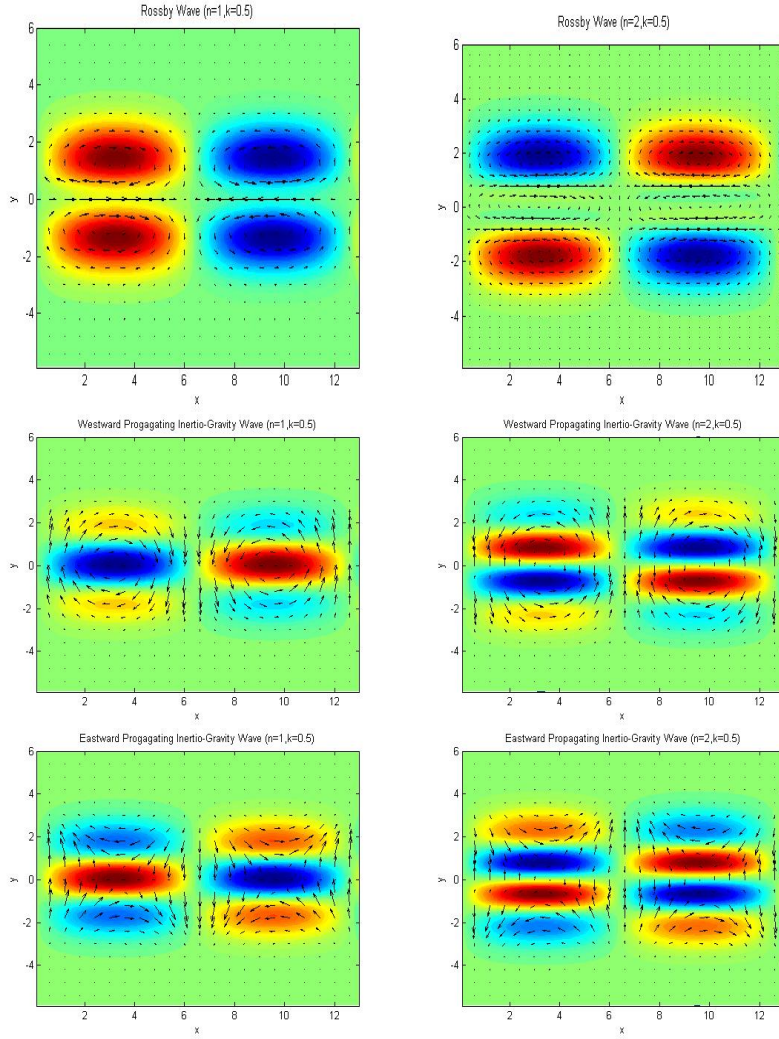


Figure 2.6: Pressure distribution (colour) and velocity vectors for  $n = 1$  mode (left) and  $n = 2$  (right) for  $k = 0.5$ . Rossby wave upper panel, westward propagating inertio-gravity wave middle panel and eastward propagating inertio-gravity wave bottom panel. Non-dimensional coordinates.

# Chapter 3

## Lee Waves

Despite of the relative smoothness of the globe, the atmosphere is so shallow that the mountains and ridges on its surface can penetrate into a significant proportion of it's depth. The atmosphere is for the most part stably stratified and thus sensitive to vertical motion, forced in this case by orography. The lee wave is a standing gravity wave where by a disturbance arising, usually from some isolated orography (e.g. a mountain), is propagated through the atmosphere via buoyancy. A stratified fluid at rest will tend to have any disturbances restored by the buoyancy force [15]. Such waves can have an impact on weather phenomena (clouds, turbulence etc.) and their development must be taken into consideration in numerical weather prediction, therefore it is important that accurate studies can be made. The Meteorological Office in the UK forecasts lee wave events for civil and military aviation, but severe gales resulting from a trapped lee wave event can also effect the surface, damaging property (e.g. Sheffield gale 16 Feb 1962)[13]. An untrapped lee wave disperses its energy vertically where it amplifies due to the decrease in density of the atmosphere with height. A trapped wave, however, is unable to disperse vertically due to a certain vertical structure of the atmosphere (see later) and amplifies via resonance with the orography underneath. [13]

### 3.1 The Linearised Boussinesq Equation Set

The derivation of the Schrödinger equation in the context of trapped lee waves follows from the linearised Boussinesq equation set ([8] pages 197-199). The Boussinesq approximation is that the density is assumed constant everywhere apart from in the buoyancy term in the vertical momentum equation. This means that the density is considered uniform and the model deals with small perturbations from this mean field, in effect removing the large static state of the atmosphere leaving only the interesting motions that we are concerned with.

We also neglect the effects of rotation, since the horizontal scales we are interested in will be small, and consider motion only in the  $x, z$  plane, with the  $x$ -axis aligned with the mean horizontal flow, to derive a diagnostic relationship between the vertical and horizontal wind perturbation fields. Therefore with  $\mathbf{v} = (u, w)$  our starting equation set will be

$$\frac{D\mathbf{v}}{Dt} + \frac{1}{\rho}\nabla p + \mathbf{g} = 0 \quad (3.1)$$

$$\nabla \cdot \mathbf{v} = 0 \quad (3.2)$$

$$\frac{D\theta}{Dt} = 0 \quad (3.3)$$

where  $\frac{D}{Dt} = \frac{\partial}{\partial t} + \mathbf{v} \cdot \nabla$ .

Now for a stratified atmosphere we assume that the basic state of horizontal wind, temperature and pressure varies only with height and thus linearise our equation set by setting

$$\rho = \rho_0 + \rho' \quad (3.4)$$

$$p = \bar{p}(z) + p' \quad (3.5)$$

$$\theta = \hat{\theta}(z) + \theta' \quad (3.6)$$

$$u = \bar{u}(z) + u' \quad w = w' \quad (3.7)$$

where the basic mean density  $\rho_0$  is constant.

We also assume that the basic state is in hydrostatic balance, that is that

$$\frac{d\bar{p}}{dz} = -\rho_0 g \quad (3.8)$$

The linearisation of equations (3.1)-(3.3) follows by substituting in equations (3.4)-(3.7) and neglecting terms which are multiples of perturbation quantities. Taking, for example the vertical momentum equation from equation (3.1) we have

$$\begin{aligned} \frac{\partial w'}{\partial t} + (\bar{u} + u', w') \cdot \nabla w' &+ \frac{1}{\rho' + \rho_0} \frac{\partial(\bar{p} + p')}{\partial z} + g \\ &\approx \frac{\partial w'}{\partial t} + \bar{u} \frac{\partial w'}{\partial x} + \frac{1}{\rho_0} \frac{d\bar{p}}{dz} \left(1 - \frac{\rho'}{\rho_0}\right) + \frac{1}{\rho_0} \frac{\partial p'}{\partial z} + g \\ &= \frac{\partial w'}{\partial t} + \bar{u} \frac{\partial w'}{\partial x} + \frac{1}{\rho_0} \frac{\partial p'}{\partial z} + \frac{\rho'}{\rho_0} g = 0 \end{aligned}$$

similarly with the rest of equations (3.1)-(3.3) so our equation set becomes

$$\frac{\partial u'}{\partial t} + \bar{u} \frac{\partial u'}{\partial x} + w' \frac{d\bar{u}}{dz} + \frac{1}{\rho_0} \frac{\partial p'}{\partial x} = 0 \quad (3.9)$$

$$\frac{\partial w'}{\partial t} + \bar{u} \frac{\partial w'}{\partial x} + \frac{1}{\rho_0} \frac{\partial p'}{\partial z} + \frac{\rho'}{\rho_0} g = 0 \quad (3.10)$$

$$\frac{\partial u'}{\partial x} + \frac{\partial w'}{\partial z} = 0 \quad (3.11)$$

$$\frac{\partial \theta'}{\partial t} + \bar{u} \frac{\partial \theta'}{\partial x} + w' \frac{d\bar{\theta}}{dz} = 0 \quad (3.12)$$

## 3.2 Lee Wave Schrödinger Equation

We can now eliminate  $p'$  from the momentum equations by taking  $\frac{\partial}{\partial z}$  of equation (3.9) and subtracting from  $\frac{\partial}{\partial x}$  of equation (3.10). This leaves us with

$$\left(\frac{\partial}{\partial t} + \bar{u} \frac{\partial}{\partial x}\right) \left(\frac{\partial w'}{\partial x} - \frac{\partial u'}{\partial z}\right) + \frac{g}{\rho_0} \frac{\partial \rho'}{\partial x} - w' \frac{d^2 \bar{u}}{dz^2} - \frac{d\bar{u}}{dz} \frac{\partial u'}{\partial x} - \frac{\partial w'}{\partial z} \frac{d\bar{u}}{dz} = 0 \quad (3.13)$$

and we cancel the final two terms via equation (3.11).

Substituting equations (3.4)-(3.6) into the definition of potential temperature  $\theta = T \left( \frac{p}{p_0} \right)^\kappa$ ,  $\kappa = -\frac{R}{c_p}$  we can find to a first approximation ([8] page 198,199)

$$\theta'/\bar{\theta} = -\rho'/\rho_0$$

via the ideal gas law,  $p = TR\rho$ .

This enables us to eliminate  $u'$  and  $\theta'$  ( $\rho'$ ) from equation (3.13). Firstly differentiate equation (3.13) with respect to  $x$ :

$$\left( \frac{\partial}{\partial t} + \bar{u} \frac{\partial}{\partial x} \right) \left( \frac{\partial^2 w'}{\partial x^2} - \frac{\partial^2 u'}{\partial x \partial z} \right) - \frac{g}{\bar{\theta}} \frac{\partial^2 \theta'}{\partial x^2} - \frac{\partial w'}{\partial x} \frac{d^2 \bar{u}}{dz^2} = 0$$

Now substituting from equation (3.11) and taking  $\frac{\partial}{\partial t} + \bar{u} \frac{\partial}{\partial x}$

$$\left( \frac{\partial}{\partial t} + \bar{u} \frac{\partial}{\partial x} \right)^2 \left( \frac{\partial^2 w'}{\partial x^2} + \frac{\partial^2 w'}{\partial z^2} \right) - \left( \frac{\partial}{\partial t} + \bar{u} \frac{\partial}{\partial x} \right) \left( \frac{g}{\bar{\theta}} \frac{\partial^2 \theta'}{\partial x^2} - \frac{\partial w'}{\partial x} \frac{d^2 \bar{u}}{dz^2} \right) = 0$$

Using equation (3.12) to simplify the second term and noting that the buoyancy frequency  $N^2 = \frac{g}{\bar{\theta}} \frac{d\bar{\theta}}{dz}$  we obtain

$$\left( \frac{\partial}{\partial t} + \bar{u} \frac{\partial}{\partial x} \right)^2 \left( \frac{\partial^2 w'}{\partial x^2} + \frac{\partial^2 w'}{\partial z^2} \right) + N^2 \frac{\partial^2 w'}{\partial x^2} - \left( \frac{\partial}{\partial t} + \bar{u} \frac{\partial}{\partial x} \right) \left( \frac{\partial w'}{\partial x} \frac{d^2 \bar{u}}{dz^2} \right) = 0$$

In the case of Lee waves it is appropriate to consider motions that are stationary relative to the ground, this means we consider  $w'$  only as a function of  $x$  and  $z$ , thus we have

$$\frac{\partial^2}{\partial x^2} \left( \frac{\partial^2 w'}{\partial x^2} + \frac{\partial^2 w'}{\partial z^2} + \frac{N^2}{\bar{u}^2} w' - \frac{w'}{\bar{u}} \frac{d^2 \bar{u}}{dz^2} \right) = 0$$

or alternatively

$$\frac{\partial^2 w'}{\partial x^2} + \frac{\partial^2 w'}{\partial z^2} + \frac{N^2}{\bar{u}} w' - \frac{w'}{\bar{u}} \frac{d^2 \bar{u}}{dz^2} = 0 \quad (3.14)$$

If we now assume a wave-like distribution of  $w$  in the horizontal, as observed in trapped lee wave events, i.e.

$$w'(x, z) = W(z)e^{ikx}$$

then equation (3.14) will become

$$\frac{d^2W}{dz^2} + (l_s^2(z) - k^2) W = 0 \quad (3.15)$$

where the Scorer parameter  $l_s(z)$  is given by

$$l_s^2(z) = \frac{N^2}{\bar{u}^2} - \frac{1}{\bar{u}} \frac{d^2\bar{u}}{dz^2}$$

Two important points should be noted at this stage, namely if the mean horizontal wind is zero at any height the Scorer parameter becomes undefined, and also at the ground the vertical wind will be zero, thus in our methods we consider only solutions where  $\Phi_0 = 0$ .

### 3.3 Analytic Scorer parameter profile

Thus to solve the lee wave problem we require a profile of the Scorer parameter to present us with the familiar problem with the horizontal wave number here taking on the role of eigenvalue. In the case of trapped lee waves, which are of interest in this study, we require a decreasing profile of  $l_s(z)$  with height. Such a profile can be obtained by observational data taken, for example, from radiosonde ascents or from the output of a forecast model. However useful studies have been made making use of analytical forms for  $l_s(z)$ . Foldvik (1962) [6] recommends that an exponential profile provides a good representation for most mid-latitude weather systems:

$$l_s(z) = l_s(0)e^{-cz} \quad (3.16)$$

where  $1/c$  is the vertical decay scale. Estimations of  $l_s(0)$  and  $c$  can be made to allow the profile to approximate observational data. We can derive solutions to equation (3.15) by making the following change of variable

$$Z = l_s(0)e^{-cz}$$

thus

$$\frac{d^2W}{dz^2} = c^2 Z^2 \frac{d^2W}{dZ^2} + c^2 Z \frac{dW}{dZ}$$

and equation (3.15) becomes

$$c^2 \left\{ Z^2 \frac{d^2 W}{dZ^2} + Z \frac{dW}{dZ} \right\} + (Z^2 - k^2) W = 0 \quad (3.17)$$

a further rescaling of  $Z = cZ^*$  allows us to write equation (3.17) as

$$Z^{*2} \frac{d^2 W}{dZ^{*2}} + Z^* \frac{dW}{dZ^*} + \left( Z^{*2} - \frac{k^2}{c^2} \right) W = 0 \quad (3.18)$$

which is Bessel's equation and has readily available solutions in the form of Bessel functions. Since we require solutions which are non-singular at the origin we must turn to Bessel functions of the first kind [1] defined as solutions to the equation

$$x^2 \frac{d^2 y}{dx^2} + x \frac{dy}{dx} + (x^2 - \alpha^2) y = 0$$

thus the Bessel function of the first kind is

$$J_\alpha[x] = \sum_{m=0}^{\infty} \frac{(-1)^m}{m! \Gamma(m + \alpha + 1)} \left( \frac{x}{2} \right)^\alpha$$

where  $\Gamma(x)$  is the Gamma function defined by

$$\Gamma(x) = \int_0^{\infty} t^{x-1} e^{-t} dt$$

Thus solutions to equation (3.18) are given by

$$w(z) = J_{k/c} \left[ \frac{l_s(0)}{c} e^{-cz} \right] \quad (3.19)$$

Notice that  $W(+\infty)$  corresponds to  $J_{k/c}(0) = 0$  as required, independent of  $k$  and  $c$ . Resonant, trapped modes are such that  $W(0) = 0$ . This equips us with an equation in  $k$  for which we have resonance

$$J_{k/c} \left[ \frac{l_s(0)}{c} \right] = 0 \quad (3.20)$$

Thus, assuming  $l_s(0)$  and  $c$  are supplied by the problem, we are able to use the bisection/secant method as described in section 1.4 to solve this equation and

converge upon allowed  $k$ . Notice that although we have an analytic means of solving for  $w$  we have no such exact formulation for the resonant horizontal wavenumbers. As such they need to be computed numerically, and this must be taken into consideration when comparing our numerical methods.

Using  $l_s(0) = 1.5$  and  $c = 0.15$  to give a quasi-realistic profile of  $l_s$  (Foldvik 1962 [6]) with height units in  $km$ , it is possible to compare the standard shooting method with the phase/amplitude model.

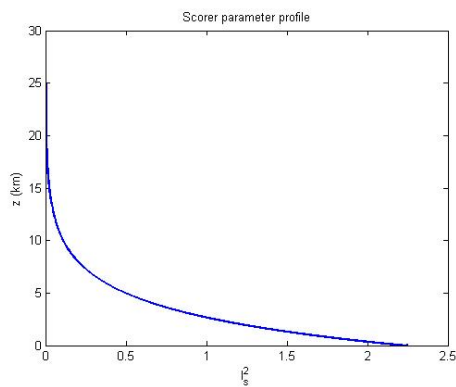


Figure 3.1: Analytic Scorer parameter profile  $l_s^2(z)$ ,  $l_s(0) = 1.5$ ,  $c = 0.15$

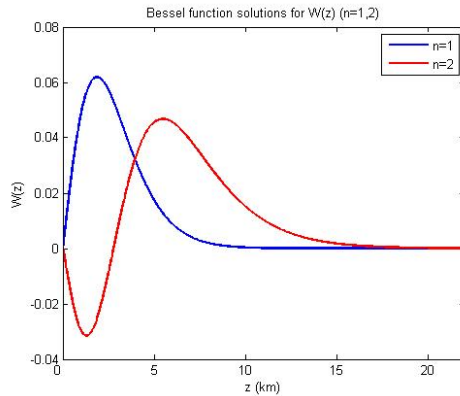


Figure 3.2: Bessel function solutions of  $W$  with exponential potential (equation (3.16))  $l_s(0) = 1.5$  and  $c = 0.15$ . Two resonant modes plotted.  $\lambda_1 = 6.9km$  and  $\lambda_2 = 13.2km$

Figure 3.2 shows the resonant modes computed by means of the bessel

function solution. In this regime we find only two resonant modes in a physically reasonable domain. The second mode with a horizontal wavelength of  $\lambda_1 = 13.2km$  is perhaps not as reasonable as the first, although in the interests of pragmatism, we shall assume that it is allowed to allow more analysis of the methods. The iterations to converge upon these modes is discussed in the following section.

### 3.3.1 Numerical Results

step size $dx$	Phase/Amplitude Error	Std Shooting Error
0.1	$2.8e-007km^{-1}$	$1.8e-007km^{-1}$
0.01	$9.0e-012km^{-1}$	$1.9e-011km^{-1}$
0.001	$1.7e-014km^{-1}$	$7.4e-015km^{-1}$

Table 3.1: Accuracy of computed wavenumber  $k$  for the phase/amplitude and shooting method compared to the secant method solution of the Bessel function initial condition equation (3.20).  $n = 1$ , wavelength =  $6.9km$ ,  $X$  integration length  $22km$ ,  $l_s(0) = 1.5$ ,  $c = 0.15$ .

step size $dx$	Phase/Amplitude Error	Std Shooting Error
0.1	$3.2e-007km^{-1}$	$6.1e-007km^{-1}$
0.01	$5.0e-012km^{-1}$	$6.1e-011km^{-1}$
0.001	$3.9e-014km^{-1}$	$4.6e-014km^{-1}$

Table 3.2: Accuracy of computed wavenumber  $k$  for the phase/amplitude and shooting method compared to the secant method solution of the Bessel function initial condition equation (3.20).  $n = 2$ , wavelength =  $13.2km$ ,  $X$  integration length  $39km$ ,  $l_s(0) = 1.5$ ,  $c = 0.15$ .

Tables 3.1 and 3.2 show the accuracy of the computed resonance wave number for the two preferred methods compared to the Bessel function so-

lution for a range of resolutions. The stopping criterion for the convergence Bessel function initial condition solver in computing the resonant wave numbers was set to machine precision (`eps`). Thus we are justified in comparing the convergence of the methods with this benchmark. As with the equatorial wave case we find these lowest modes being of comparable accuracy, with a marginal loss of accuracy in the direct shooting method in the higher mode. It must be noted that the integration length is essential for accurate computations in both methods, which is not an issue with an analytic profile, however when the Scorer parameter profile is taken from observational data, e.g. radiosonde ascent, this will restrict the interval we solve over and thus restrict the computation of higher modes.

Mode	Phase/Amplitude	Std Shooting	Bessel Method
$n$	Iterations	Iterations	Iterations
1	11	14	9
2	8	14	9

Table 3.3: Number of iterations for convergence for the phase/amplitude and shooting method compared to the secant method solution of the Bessel function initial condition equation (3.20).  $X$  integration length as in table 3.1 with  $dz = 1m$ ,  $l_s(0) = 1.5$ ,  $c = 0.15$ .

Table 3.3 includes the iterations required for convergence of the three techniques under consideration, namely phase/amplitude, the direct shooting method and the Bessel solution (note this includes the bisection iterations). As mentioned previously the Bessel solver had machine precision as its stopping criterion compared to the phase/amplitude and direct shooting methods which both have the stopping criterion  $\epsilon = 10^{-7}$

Here we find again the phase/amplitude converging with fewer iterations than the direct shooting method. In the higher mode the phase/amplitude method converges with fewer iterations than the Bessel function solution (by means of the bisection and secant method) although not to the same level of accuracy.

It is the author's opinion that the phase/amplitude method, while being consistently numerically accurate, also allows for easier searching of the resonant modes. Both the direct shooting and Bessel function techniques require significantly more user input to specify the ranges of wave number to search for resonant mode, with no guarantee of success. However by isolating the mode by  $k$  in the boundary condition, the phase/amplitude method requires no searching and will converge with a standard guess over all modes. For instance the wave numbers for  $n = 1$  and  $n = 2$  modes were  $k = 0.91$  and  $k = 0.48$  so initial intervals for  $k$  were  $[0.5, 1]$  and  $[0.2, 0.5]$  respectively. These are by no means large intervals and a systematic procedure was necessary to establish them. By contrast the phase/amplitude method was given an initial guess of  $k = 0.1$  and converged in both cases with boundary condition,  $\Phi(X) = n\pi$  ( $n = 1, 2$ ), isolating the modes.

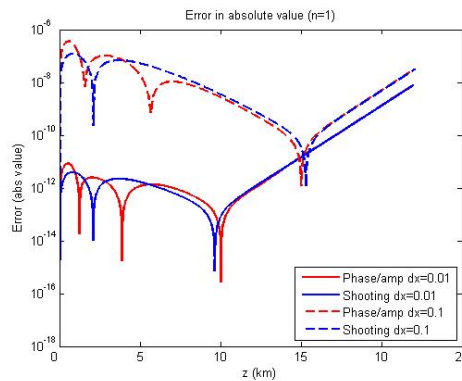


Figure 3.3: Absolute value of the error of the computed solution,  $W(z)$  from the phase/amplitude method (red curves) and the direct shooting method (blue curves) when compared to Bessel function solution. Dotted curves step size  $dx = 0.1km$  and solid  $dx = 0.01km$ .  $n = 1$ , wavelength =  $6.9km$ , integration length  $X = 22km, l_s^2(0) = 1/5, c = 0.15$ . (logarithmic axis)

Figures 3.3 and 3.4 further show the accuracy of the full solution from the two numerical methods (again normalised), for the modes in question, compared to the Bessel function solution. The two methods are of comparable accuracy, with the phase/amplitude method becoming slightly improved

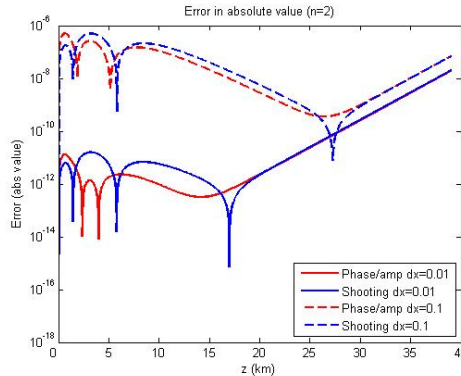


Figure 3.4: Absolute value of the error of the computed solution,  $W(z)$  from the phase/amplitude method (red curves) and the direct shooting method (blue curves) when compared to Bessel function solution. Dotted curves step size  $dz = 0.1\text{km}$  and solid  $dz = 0.01\text{km}$ .  $n = 2$ , wavelength =  $13.2\text{km}$ , integration length  $X = 39\text{km}$ ,  $l_s^2(0) = 1/5$ ,  $c = 0.15$ . (logarithmic axis)

in the higher mode, however the loss of accuracy at the end of the interval dominates for both methods.

### 3.4 Observed Scorer parameter profiles

Despite the analytic Scorer parameter profile providing a reasonable approximation and allowing a comparison with a known solution, it is preferable to obtain a more realistic form of  $l_s(z)$  i.e. an observed profile. Shutts (1997) [13] describes making use of equation (3.15) in a code designed to forecast trapped lee wave events. This work uses second order finite differencing and a direct shooting method to calculate resonant modes, thus an improvement can be made by using the phase/amplitude method to perform this computation.

To employ the phase/amplitude method on a discrete profile, the observed data will need to be interpolated to define the profile at the desired resolution. This is achieved by means of cubic splines (MATLAB `spline` function) where a piecewise polynomial (cubic) representation interpolates between the data

nodes. In some instances a smoothing process may also need to be carried out to obtain a sufficiently smooth and continuous representation of the Scorer parameter profile.

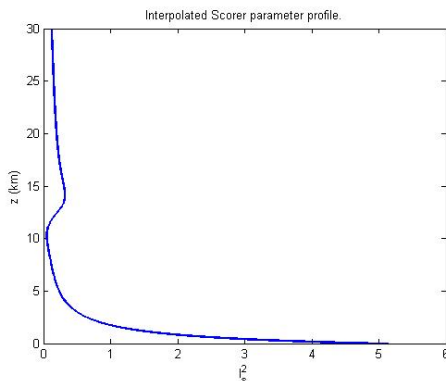


Figure 3.5: Cubic spline interpolated Scorer parameter profile ( $l_s^2(z)$ ), resolution  $dz = 1m$

Figure 3.5 shows the interpolated data. Observations of temperature, wind speed, pressure and height from a radiosonde sounding were used to calculate the Scorer parameter profile every  $250m$  through the atmosphere to an altitude of  $30km$ . The spline interpolation has improved the resolution to  $1m$ . It is clear from this profile why the exponential form (equation (3.16)) is a reasonable approximation, however it must be noted that not all instances of lee waves have such a smooth Scorer parameter profile. The phase/amplitude and direct shooting methods were employed to search for resonant modes with this atmospheric profile. The phase/amplitude initial conditions in this case are set via a finite difference we have only a discrete representation. Taking an initial guess for  $k$ , only one resonant mode is found, that being the lowest mode with a wavelength of  $7.89km$  with  $dx = 0.01km$ . Interestingly decreasing the resolution to  $dx = 0.1km$  we find that this wavelength becomes  $8.15km$ . The reasons for this are not obvious, but maybe attributed to the spline interpolation, where the profile is extrapolated to the ground. Also it was found for the lower resolution that the two methods agreed to ten decimal places while the lower resolution only to six.

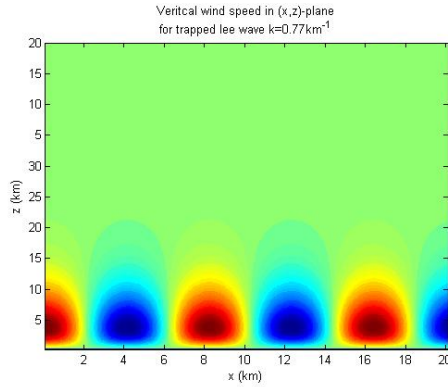


Figure 3.6: Solution of  $w'(x, z)$  of resonant trapped lee wave distribution for observed Scorer parameter profile, resolution  $dz = 100m$

Figure 3.6 shows the distribution of vertical wind perturbation in the  $(x, z)$ -plane given by

$$w'(x, z) = W(z)e^{ikx}$$

with  $W(z)$  computed from the phase/amplitude method for resonant wavelength  $7.89km$ . This plot exhibits the familiar lee wave pattern that is observed downstream of mountain ranges when resonance occurs; the ascent and descent that forms the wave cloud patterns.

As mentioned in the introductory paragraph about lee waves, the trapped lee waves are amplified through resonance with the underlying orography. Thus in any operational lee wave finding code, this will have to be taken into account to specify the lee wave amplitude in particular case studies but is beyond the scope of this work (see [13]).

## Conclusion

This work has involved a detailed study of the benefits of the phase/amplitude method over its contemporary numerical techniques in the solution of the time independent Schrödinger equation. This involved solving ODE's for phase and amplitude via a fourth order finite difference scheme (Runge-Kutta) and using a shooting method to fix the end boundary condition via Newton iteration. The boundary condition is formulated "at infinity" such that we have decaying behaviour in the region of negative potential, giving the solutions required in the study of atmospheric and oceanic trapped waves.

One set wave motions studied were trapped equatorial Rossby and inertio-gravity waves via a  $\beta$ -plane approximation, where analytic solutions exist [10]. The Schrödinger equation involves the meridional component of wind velocity and the potential here takes on a quadratic form, whereby the variation of coriolis force acts to trap wave motions about the equator. The eigenvalue of the problem is an expression involving the zonal frequency and wavenumbers. Exact solutions exist in the form of parabolic cylinder functions in this case and eigenvalues take odd integer values.

The other set of wave motions considered is that of trapped lee waves, or mountain waves, where stationary, internal gravity waves are forced by the orography. The derivation of the Schrödinger equation here involved the linearisation of the Boussineq equation set, under stationary conditions such that dependent variables are eliminated in favour of vertical wind speed. The resulting potential is commonly referred to as the Scorer parameter, a function of horizontal wind speed and static stability, with eigenvalue the horizontal wave number squared and under conditions where this decays with height trapped wave resonances occur. The work considers an analytic profile of Scorer parameter where known solutions exist in the form of Bessel functions, and accuracy and convergence comparisons are again made. Also a Scorer parameter profile involving observed data is interpolated and the nu-

merical techniques are employed to solve and compute the resonance modes.

The results from the computations in the cases described above allow some analysis of the numerical techniques. It was found that the phase/amplitude method was more effective for higher modes than its counterpart direct shooting method, although it struggled somewhat with the lower modes. In the case of equatorial waves the lowest mode was an order of magnitude less accurate than the direct shooting method but in the lee wave case (analytic Scorer profile) the lowest modes were of comparable accuracy. The phase/amplitude method also showed an improvement in searching for resonant modes. The direct shooting approach requires a systematic method to search for the resonant modes, where the phase/amplitude method presents a more elegant method of isolating modes via the boundary condition.

It would be possible to extend the work on equatorial waves, using the phase/amplitude method, to cover motions involving the full variation of the coriolis force about the equator, using spherical geometry. In this case the potential takes on a much more complex form and no known analytic solutions exist, thus the use of efficient and accurate numerical techniques is the only method of solving (see Erlick et. al. [5]).

The phase/amplitude method could also be used in an operational lee wave forecasting code, where resonant modes can be computed from observed profiles of the atmosphere and orographic observations will approximate amplitudes. (see Shutts [13])

## **Acknowledgments**

This work would not have been possible without the supervision of Rémi Tailleaux whose support, patience and advice has been invaluable. I would also like to thank Bob Lucas for his help with diagrams. The financial support provided by the Natural Environment Research Council for this MSc has been extremely important in the completion of this work.

# Bibliography

- [1] Abramowitz M., Stegun I.A., 1972: *Handbook of Mathematical Functions with Formulas, Graphs and Mathematical Tables*. National Bureau of Standards. Applied Mathematics Series- 55. 19.13
- [2] Bateman, H., 1953: *Higher Transcendental Functions*. Volume II McGraw-Hill Book Company. 8.2
- [3] Burden, R.L., Faires, J.D. 1997: *Numerical Analysis*. Sixth Edition. Brooks/Cole Publishing Company.
- [4] Cheney, W., Kincaid, D., 1996: *Numerical Analysis. Mathematics of Scientific Computing*. Second Edition. Brooks/Cole Publishing Company.
- [5] Erlick, C. et.al 2007: Linear waves in a symmetric equatorial channel. *Q. J. R. Meteorol. Soc.* 133:571-577.
- [6] Foldvik, A. 1962: Two-dimensional mountain waves - a method for the rapid computation of lee wavelengths and vertical velocities. *Q. J. R. Meteorol. Soc.* 88: 271-285.
- [7] Gill, A.E., 1982: *Atmosphere Ocean Dynamics*. International Geophysics Series. Volume 20. Academic Press. Sections 11.6,11.8
- [8] Holton J.R., 2004: *An Introduction to Dynamic Meteorology*. Fourth Edition. International Geophysics Series. Volume 88. Elsevier Academic Press. Sections 7.4.2, 11.4

- [9] Korsch, H. J., Laurent, H., 1981: Milne's differential equation and numerical solutions of the Schrödinger equation I. Bound-state energies for single- and double-minimum potentials. *J. Phys. B: At. Mol. Phys.* 14 (1981) 4214-4230.
- [10] Matsuno, T., 1966: Quasi-geostrophic motions in the equatorial area. *J. Met. Soc. Japan* 44: 24-42.
- [11] Milne W.E., 1930: The Numerical Determination of Characteristic Numbers. *Physical Review. Volume 35.* 863-867.
- [12] Smith, R. B. 1979: *The Influence of Mountains on the Atmosphere.* Advances in geophysics. Volume 21. 87-230
- [13] Sutts, G. 1997: Operational lee wave forecasting. *Meteorol. App.* 4, 23-25 (1997)
- [14] Trench W.F., 2000: *Elementary Differential Equations.* Brooks/Cole Publishing Company.
- [15] Wurtele M.G., Sharman R.D., Datta A., 1996: Atmospheric Lee Waves. *Annu. Rev. Fluid Mech.* 1996.28/429-76.
- [16] Yuan J M, Lee S Y, Light J C, 1974: Reduced Fermion density matrices. II. Electron density of Kr. *J. Chem. Phys.* 61 3394-400.

# Appendix A

## MATLAB functions

### A.1 Phase/Amplitude routine

The following MATLAB code contains all functions used in the phase/amplitude method. The main routine, “PAsolve” takes as input interval length (assumed, as in cases discussed to begin at 0, i.e.  $[0, X0]$ ), first guess at eigenvalue  $\lambda$ , mode  $n$ ,  $\Phi_0$  set to either 0 or  $\pi/2$  to recover odd/even solutions, and step size  $dx$ . The outputs are eigenvalue, solution  $y(x)$ , amplitude and phase. Initial conditions, in the case of analytic potentials are best input by hand, where derivatives of potential are required. In the case of non-analytic potentials, this can be approximated via finite difference.

An example of the calling procedure, here for the equatorial case, for the  $n = 3$  mode would be

```
[lambda, v, A, phi]=PAsolve(7,10,2,pi/2,0.01)
```

with step size 0.01.

```
1
2 function [lambda,Y,A1,phi]=PAsolve(X0,L,n,phi_0,dx)
3
4 %%%%%%%%%%%%%%%%%%%%%%%%%%%%%%%%%%%%%%%%%%%%%%%%%%%%%%%%%%%%%%%%%%%%%%%%%%
```

```

5 % msolve function for phase/amplitude method
6 %
7 % To be used in conjunction with RKs 4th
8 % order Runge-Kutta solver and associated functions.
9 %
10 % Inputs are interval size, initial guess for eigenvalue
11 % Phi_0, n mode, and resolution dx.
12 %
13 % Outputs eigenvalue, solution, phase and amplitude
14 %
15 %%%%%%%%%%%%%%%%%%%%%%%%%%%%%%%%%%%%%%%%%%%%%%%%%%%%%%%%%%%%%%%%%%%%%%%%%
16
17
18 N=X0/dx; %number of steps
19 e=0.000001; %shooting method tolerance
20 a=1; %iteration step
21 lambda(1)=L;
22 while (a<20) %iteration limit to prevent infinite loop
23
24     A1(1)=(V(0,dx,lambda(a)))^(-0.25); %initial conditions
25     A2(1)=0; %equatorial case, derivative BC =0
26     phi(1)=0;
27
28
29     for k=2:N %solver loop
30         %RK4 call
31         [A1(k),A2(k),phi(k)]=RKs(A1(k-1),A2(k-1),phi(k-1)
32         ,k-2,dx,lambda(a));
33     end
34
35 %break out of iteration loop once tolerance satisfied
36 if (abs(A1(N)*sin(phi(N)-phi_0))<e)
37     %compute Y final solution
38     for K=1:N
39         Y(K)=A1(K)*sin(phi(K)-phi_0);
40         %Y(n,K)=(1/(sqrt(A1(K))))*sin(phi(K));
41     end
42     Y=Y/norm(Y);

```

```

43         break
44
45     end
46
47
48
49     r(a)=(phi(N)-phi_0)-n*pi); %compute residue
50
51     %dR/d Lambda by composite trapezium rule
52     D(1)=0;
53     for K=2:(N-1)
54         D(K)=(D(K-1)+(dx)*(d(A1(K),phi(K),phi(N)))));
55     end
56     D1=D(N-1)+(dx/2)*(d(A1(N),phi(N),phi(N)))
57         +sin(2*phi(N))/(4*V(0,dx,lambda(a)));
58
59     %update lambda: Newton iteration.
60
61     %secant method commented out
62     % if (n==1)
63     % lambda(2)=lambda(1)+0.001;
64     %else
65     % D=(r(n)-r(n-1))/(lambda(n)-lambda(n-1));
66     lambda(a+1)=lambda(a)-r(a)/D1;
67     % end
68
69
70     a=a+1;
71 end
72 end
73
74
75
76
77 function [a1,a2,phi]=RKs(A1,A2,Phi,i,dx,lambda)
78
79 %%%%%%%%%%%%%%%%%%%%%%%%%%%%%%%%%%%%%%%%%%%%%%%%%%%%%%%%%%%%%%%%%%%%%%%%%
80 %

```

```

81 %      RK4 solver for system of equations in
82 %          phase/amplitude method
83 %
84 %      A1,A2,Phi from previous step,
85 %      i step index,
86 %      dx step length,
87 %      l eigenvalue.
88 %
89 %%%%%%%%%%%%%%%%%%%%%%%%%%%%%%%%%%%%%%%%%%%%%%%%%%%%%%%%%%%%%%%%%%%%%%%%%
90
91 j1=dx*(f(A1));
92 k1=dx*A2;
93 l1=dx*g(A1,A2,i,dx,lambda);
94
95 j2=dx*(f(A1+k1/2));
96 k2=dx*(A2+l1/2);
97 l2=dx*g(A1+k1/2,A2+l1/2,i+1/2,dx,lambda);
98
99 j3=dx*(f(A1+k2/2));
100 k3=dx*(A2+l2/2);
101 l3=dx*g(A1+k2/2,A2+l2/2,i+1/2,dx,lambda);
102
103 j4=dx*(f(A1+k3));
104 k4=dx*(A2+l3);
105 l4=dx*g(A1+k3,A2+l3,i+1,dx,lambda);
106
107 j=(1/6)*(j1+2*j2+2*j3+j4);
108 k=(1/6)*(k1+2*k2+2*k3+k4);
109 l=(1/6)*(l1+2*l2+2*l3+l4);
110
111
112 a1=A1+k;
113 a2=A2+l;
114 phi=Phi+j;
115
116
117 end
118

```

```

119
120 function G=g(A1,A2,i,dx,lambda)
121 %function for RHS of second derivative
122
123 %solving for phase
124 %G=(3/2)*(A2^2/A1)-2*A1*(A1^2-V(i,dx,lambda,c));
125
126 %solving for amplitude
127 G=1/(A1^3) -V(i,dx,lambda)*A1;
128
129 end
130
131
132
133 function v=V(i,dx,lambda)
134 %potential
135
136 v=-(i*dx)^2+lambda; %equatorial potential
137
138 end
139
140
141 function F=f(x)
142 %function for phase solution
143
144 %F=x; %solving for phase
145 F=1/(x^2); %solving for amplitude
146 end
147
148
149 function D=d(A,phi,phiX)
150 %function to evaluate integrand in trapezium composite rule
151 % for dR/d lambda
152
153 D=(A^2)*((sin(phi-phiX))^2);
154 end

```

## A.2 Direct Shooting Method

Commented MATLAB code follows for the direct shooting method via bisection and secant methods. Function “Ssolve” takes inputs of integration length, X0, eigenvalue search interval  $[\lambda_0, \lambda_1]$  and step size dx. The function outputs eigenvalue  $\lambda$  and normalised solution Y. This routine calls a similar RK4 solver as PAsolve, and uses the same function ‘V’ for potential. The initial conditions again have to be manually changed to recover odd/even solutions. This could be incorporated into the input data for the routine however.

An example of calling this routine would be

```
[lambda, v]=Ssolve(7, 6.5, 8,0.01);
```

to recover the same example as the phase/amplitude method.

```
1 function [lambda,Y]=Ssolve(X0,lambda0,lambda1,dx)
2
3 %%%%%%%%%%%%%%%%%%%%%%%%%%%%%%%%%%%%%%%%%%%%%%%%%%%%%%%%%%%%%%%%%%%%%%%%%
4 %   msolve function for phase/amplitude method
5 %
6 %   To be used in conjunction with RKs 4th
7 %   order Runge-Kutta solver and associated functions.
8 %
9 %%%%%%%%%%%%%%%%%%%%%%%%%%%%%%%%%%%%%%%%%%%%%%%%%%%%%%%%%%%%%%%%%%%%%%%%%
10
11
12 X=X0/dx;           %number of steps
13 e=0.000001;       %shooting method tolerance
14 n=2;              %iteration step
15 %lambda(1)=lambda0; %initial guess for lambda
16
17
18 %%%%%%%%%%%%%%%%%%%%%%%%%%%%%%%%%%%%%%%%%%%%%%%%%%%%%%%%%%%%%%%%%%%%%%%%%
19 %   Bisection iterations
```

```

20 %%%%%%%%%%%%%%%%%%%%%%%%%%%%%%%%%%%%%%%%%%%%%%%%%%%%%%%%%%%%%%%%%%%%%%%%%
21
22     Y1(1)=0; %initial conditions
23     Y2(1)=1;
24
25     for K=2:X %solver loop
26
27         %RK4 call
28         [Y1(K),Y2(K)]=
29         RKS1(Y1(K-1),Y2(K-1),K-2,dx,lambda0);
30     end
31
32     y1(1)=0; %initial conditions
33     y2(1)=1;
34
35     for K=2:X %solver loop
36
37         %RK4 call
38         [y1(K),y2(K)]=
39         RKS1(y1(K-1),y2(K-1),K-2,dx,lambda1);
40     end
41
42
43     if (sign(Y1(X))==sign(y1(X)))
44         %break out of loop if solution not in interval
45         'poor interval'
46         lambda=0;
47         return
48     end
49
50     for k=1:3
51         lambda1
52         lambda0
53         lambda2=lambda0+(lambda1-lambda0)/2;
54         YY1(1)=0; %initial conditions
55         YY2(1)=1;
56
57     for K=2:X %solver loop

```

```

58
59         %RK4 call
60         [YY1(K),YY2(K)]=
61         RKS1(YY1(K-1),YY2(K-1),K-2,dx,lambda2);
62     end
63     %update interval
64     if (sign(y1(X))==sign(YY1(X)))
65         lambda1=lambda2;
66         y1(X)=YY1(X);
67     else
68         lambda0=lambda2;
69         Y1(X)=YY1(X);
70     end
71 end
72
73
74 lambda(2)=lambda1;
75 lambda(1)=lambda0;
76
77 %%%%%%%%%%%%%%%%%%%%%%%%%%%%%%%%%%%%%%%%%%%%%%%%%%%%%%%%%%%%%%%%%%%%%%%%%
78 %   Secant iterations
79 %%%%%%%%%%%%%%%%%%%%%%%%%%%%%%%%%%%%%%%%%%%%%%%%%%%%%%%%%%%%%%%%%%%%%%%%%
80
81 while (n<20)
82     %iteration limit to prevent infinite loop
83
84     Y1(n,1)=0; %initial conditions
85     Y2(1)=1;
86
87     for K=2:X %solver loop
88
89         %RK4 call
90         [Y1(n,K),Y2(K)]=
91         RKS1(Y1(n,K-1),Y2(K-1),K-2,dx,lambda(n));
92     end
93
94     %secant method operations
95     D=(Y1(n,X)-Y1(n-1,X))/(lambda(n)-lambda(n-1));

```

```

96         lambda(n+1)=lambda(n)-Y1(n,X)/D;
97
98
99         %break out of iteration loop once tolerance satisfied
100        if (abs(Y1(n,X))<e)
101
102            Y=Y1(n,:)/norm(Y1(n,:)); %normalise solution
103
104            break
105        end
106
107
108        n=n+1;
109    end
110
111
112    function [y1,y2]=RKS1(Y1,Y2,n,dx,l)
113
114    %%%%%%%%%%%%%%%%%%%%%%%%%%%%%%%%%%%%%%%%%%%%%%%%%%%%%%%%%%%
115    %
116    %     RK4 solver for system of equations
117    %         in shooting method
118    %
119    %     Y1,Y2 from previous step,
120    %     i step index,
121    %     dx step length,
122    %     l eigenvalue.
123    %
124    %%%%%%%%%%%%%%%%%%%%%%%%%%%%%%%%%%%%%%%%%%%%%%%%%%%%%%%%%%%
125
126    k1=dx*Y2;
127    l1=dx*g1(Y1,n,dx,l);
128
129    k2=dx*(Y2+l1/2);
130    l2=dx*g1(Y1+k1/2,n+1/2,dx,l);
131
132    k3=dx*(Y2+l2/2);
133    l3=dx*g1(Y1+k2/2,n+1/2,dx,l);

```

```

134
135 k4=dx*(Y2+l3);
136 l4=dx*g1(Y1+k3,n+1,dx,l);
137
138 k=(1/6)*(k1+2*k2+2*k3+k4);
139 l=(1/6)*(l1+2*l2+2*l3+l4);
140
141
142 y1=Y1+k;
143 y2=Y2+l;
144
145
146 end
147
148 function G=g1(m1,i,dx,l)
149 % RHS of ODE
150 G=-V(i,dx,l)*m1;
151 end
152 end

```

### A.3 Matrix Eigenvalue Method

This code creates the matrix and finds eigenvalues and vectors via MATLAB's "eig" function. Inputs in this routine are interval length  $X_0$  and resolution  $dx$ , and outputs are eigenvalue and solution. Note that high resolutions are computationally expensive.

This is called simply by

$$[\text{Lambda},v]=\text{gsolve}(7,0.01)$$

```

1 function [lambda,Y]=gsolve(X0,dx)
2
3 X=X0/dx-1;
4

```

```

5 %initialise matrix A where AY=lambdaY
6 A(1,1)=-V(1,dx,0,0)-2/dx^2;
7 A(1,2)=1/dx^2;
8 A(2,1)=1/dx^2;
9 A(2,2)=-V(2,dx,0,0)-2/dx^2;
10
11 for i=3:X
12     A(i,i)=-V(i,dx,0,0)-2/dx^2;
13     A(i-1,i)=1/dx^2;
14     A(i,i-1)=1/dx^2;
15
16 end
17
18 [Y,lambda]=eig(A);
19
20 end

```

## A.4 Bessel function

This routine computes resonant modes via the Bessel function initial condition for the analytic Scorer parameter profile discussed with a combination of bisection method and secant iterations. Routine takes inputs of wavenumber interval ( $[k_0, k_1]$ ), step size  $dx$ , and interval length  $X_0$ . Outputs are normalised solutions and resonant wave number  $k$ . This routing is called by

```
[w,k]=besolve(0.2,0.5,0.01,39);
```

```

1 function [w,k]=besolve(k0,k1,dx,X0)
2
3 X=X0/dx;
4 e=0.000000000000000001;
5 n=2;
6 ls=1.5;
7 c=0.15;

```

```

8 p=0;
9
10
11 %%%%%%%%%%%%%%%%%%%%%%%%%%%%%%%%%%%%%%%%%%
12 % Search for resonant modes
13
14 % Bisection iterations
15 %%%%%%%%%%%%%%%%%%%%%%%%%%%%%%%%%%%%%%%%%%
16 z0=besselj(k0/c,ls/c);
17 z1=besselj(k1/c,ls/c);
18
19 if (sign(z0)==sign(z1))
20     'poor interval'
21     k=0;
22     return
23 end
24
25 for k=1:3
26
27     k2=k0+(k1-k0)/2;
28     z2=besselj(k2/c,ls/c);
29
30     if (sign(z1)==sign(z2))
31         k1=k2;
32         z1=z2;
33     else
34         k0=k2;
35         z0=z2;
36     end
37 end
38
39
40 k(2)=k1;
41 k(1)=k0;
42
43 %%%%%%%%%%%%%%%%%%%%%%%%%%%%%%%%%%%%%%%%%%
44 % Secant iterations
45 %%%%%%%%%%%%%%%%%%%%%%%%%%%%%%%%%%%%%%%%%%

```

```

46 while (n<20)
47
48     D=(besselj(k(n)/c,ls/c)-besselj(k(n-1)/c,ls/c))/(k(n)-k(n-1));
49     k(n+1)=k(n)-besselj(k(n)/c,ls/c)/D;
50
51     n=n+1;
52
53     if (abs(k(n)-k(n-1))<e)
54         K=k(n);
55         break
56     end
57 end
58
59 %compute solution via bessel funtion
60 for i=0:X-1
61     [w(i+1),ierr]=besselj(k(n)/c,(ls/c)*exp(-c*i*dx));
62
63 end
64 w=w/norm(w); %normalise solution

```